Towards a better understanding of African topography: a review of passive-source seismic studies of the African crust and upper mantle

Stewart Fishwick and Ian D. Bastow

Email alerting service	click here to receive free e-mail alerts when new articles cite this article
Permission request	click here to seek permission to re-use all or part of this article
Subscribe	click here to subscribe to Geological Society, London, Special Publications or the Lyell Collection

---

Notes

Lyell
Collection

Towards a better understanding of African topography: a review of passive-source seismic studies of the African crust and upper mantle

STEWART FISHWICK[1]* & IAN D. BASTOW[2]

[1]*Department of Geology, University of Leicester, University Road, Leicester, LE1 7RH, UK*

[2]*Department of Earth Sciences, University of Bristol, Wills Memorial Building,
Queen's Road, Bristol BS8 1RJ, UK*

*Corresponding author (e-mail: sf130@le.ac.uk)

Abstract: Explaining the cause and support of Africa's varied topography remains a fundamental question for our understanding of the long-term evolution of the continent. As geodynamical modelling becomes more frequently used to investigate this problem, it is important to understand the seismological results that can be incorporated into these models. Crustal thickness estimates are crucial for calculating components of topography that are isostatically compensated. Variations in seismic velocity help constrain variations in subsurface temperature and density and thus buoyancy; measurements of anisotropy can also be used to determine the contribution of the mantle flow field to dynamic topography. In this light, we review the results of passive seismic studies across Africa. At the continental scale there are significant differences in crustal models, meaning large uncertainties in corrections for isostatic topography. In east Africa, multiple seismic experiments have provided firm constraints on crustal and mantle structure. Tomographic images illuminate a broad (*c.* 500 km wide) low-velocity region in the upper mantle, with possible connection to the African Superplume in the lower mantle. These observations, alongside the variations in radial anisotropy, strongly suggest that the mantle flow field contributes significantly to the uplift of the region. Beneath southern Africa, low velocities are observed near the base of the continental lithosphere; the depth to transition zone discontinuities however suggests that they are not linked to the superplume beneath. It is thus less clear what role the sublithospheric mantle plays in supporting the region's high topography. Many of Africa's secondary topographic features (e.g. Atlas, Hoggar, Bie Dome) are underlain by slow velocities at depths of 100–150 km and are adjacent to rapid changes in lithospheric thickness. Whether these variations in lithospheric structure promote small-scale convection or simply guide the larger-scale mantle flow field remains ambiguous.

Forty years after the advent of plate tectonic theory, while the vertical motion of the oceanic plates can be explained by relatively simple arguments concerning their age and thermal structure (McKenzie 1978) the vertical movements in continental regions often remain a matter of considerable debate. For example, for a region surrounded by mostly extensional plate boundaries there is significant topography on the African continent. The dominant first-order feature is the near bimodal topography described by Doucouré & de Wit (2003): elevated topography (*c.* 500–3000 m) is observed in eastern and southern Africa, while lower topography occurs in western and central Africa and towards the north-eastern (Egyptian) margin of the continent (Fig. 1). Superimposed on these long-wavelength structures are a series of basins and swells (Fig. 1), famously described by Holmes (1944). In northern Africa the swells are frequently topped by relatively young (*c.* 35 Ma–Recent) volcanism (e.g. Hoggar,

Tibesti, Fig. 1) suggesting a link to elevated mantle temperatures and dynamic support. In the south, swells are also observed on top of the generally high topography (e.g. Namibia, Bie; Fig. 1) but in these regions are not always associated with recent volcanism. A simple correlation between hotspot tectonism and uplift is therefore not necessarily applicable continent-wide. The timing and cause of Africa's considerable topography thus remains a matter of continued debate.

In his work *The African Plate*, Burke (1996) presented the view that the majority of African topography, including the Great Escarpment, has been formed during the last *c.* 30 Ma. One indication for this young continent-wide uplift has come from interpretations of the correlations of an African surface defined using geomorphological evidence. Secondly, the prominent Oligocene unconformity observed in seismic reflection data all around the continental margin is compelling evidence that uplift commenced around this time
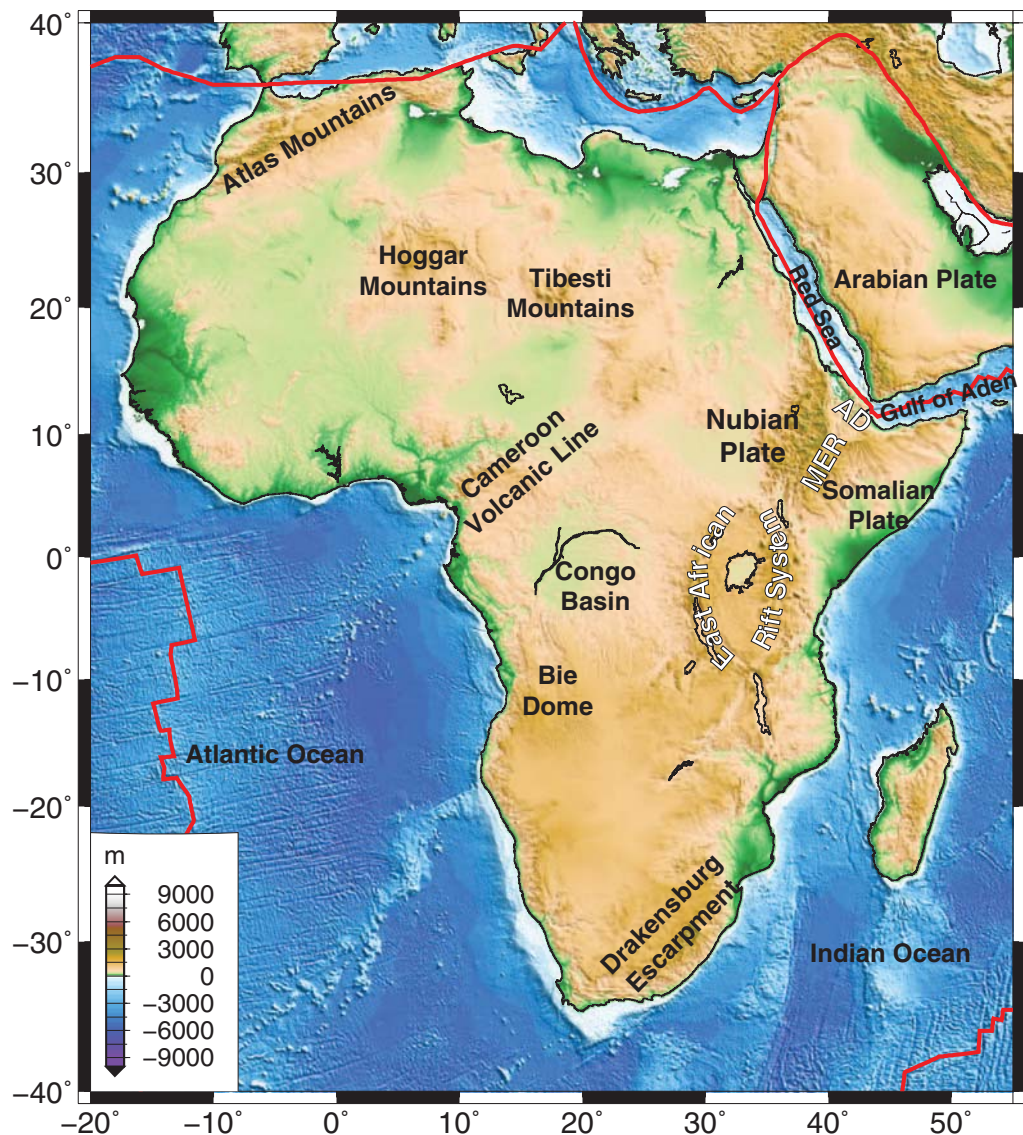
Fig. 1. Location map of Africa showing major tectonic features superimposed on regional topography (MER, Main Ethiopian Rift; AD, Afar Depression). Red lines are major plate boundaries.

(e.g. Burke 1996). Roberts & White (2010) estimate uplift histories from river profiles for a number of regions in Africa; they also suggest that significant uplift has occurred since 30–40 Ma. The timing, however, is not uniform across the continent, with recent, rapid, localized uplift occurring in regions such as the Bie Dome (Fig. 1).

In contrast, others believe that a significant part of the high African topography has a much older history. Doucouré & de Wit (2003) attempt to reconstruct the Mesozoic topography of Africa by removing the topographic effect of features known to be of Cretaceous age or younger. They observe that the bimodality of African topography was already in place in the Early Mesozoic. Significant evidence for a Mesozoic timing of the uplift comes in the form of apatite fission-track thermochronology. De Wit (2007) reviews the various apatite fission track studies alongside offshore stratigraphic studies to suggest that denudation across southern Africa operated on a wide scale (>1000 km) during the Cretaceous. Are the inferred

Mesozoic and Cenozoic histories incompatible with each other, or simply a result of differing techniques being sensitive to specific time periods?

The tectonic and geodynamic processes relating to topographic variation also appear to be variable. Collisional processes, commonly associated with regions of high topography, are the predominant factor only in the Atlas mountains (Fig. 1) of north-western Africa (e.g. Frizon de Lamotte *et al.* 2000); even in this region, however, the high topography has also been associated with convective upwelling of the underlying mantle (e.g. Teixell *et al.* 2005). Elsewhere, other factors such as the emplacement of volcanic rock at the surface during hotspot tecton-ism, crustal thinning and rift flank flexure during extensional tectonics (e.g. the East African Rift or EAR) are likely to contribute to the development of Africa's variable topography (Fig. 1).

Are all these parts of the African plate presently in a state of isostatic equilibrium, or do regions require dynamic components towards the support of the topographic variations? The classical view of isostasy can be separated into two end-member models: Airy and Pratt. In Airy isostasy, the excess mass of high topography is compensated by a thickened root of low-density material relative to the surroundings. In contrast, in the Pratt model there is no thickening of the root; high topography is compensated instead by a lower-density column directly beneath. In order to assess the cause of any isostatic support, it is therefore necessary to know both the crustal thickness and density. Depending on the choice of compensation depth, variations in the lithospheric mantle density must also be considered (see e.g. Crosby *et al.* 2010).

If the topography is not isostatically supported, alternatives include regional support due to the strength of the lithosphere or a dynamic mantle component to the support. Many of Africa's domal regions appear to have a thin (<40 km) effective elastic plate thickness (Pérez-Gussinyé *et al.* 2009), so flexural support appears an unlikely can-didate to explain the first-order topographic obser-vations. Dynamic support, or dynamic topography, will occur when flow (caused by density variations within the Earth's mantle) interacts with the surface layer (for a recent review see Braun 2010). If there are dynamic components to the support of Africa's high topography, are these dominated by perturbations in the deep mantle (e.g. Lithgow-Bertelloni & Silver 1999; Gurnis *et al.* 2000), more localized asthenospheric upwellings (e.g. King & Ritsema 2000; Montagner *et al.* 2007; Al-Hajri *et al.* 2009) or a combination of both?

Crustal thickness and density, mantle density and temperature and flow direction are therefore of first-order importance in understanding topogra-phy. Serendipitously, many of these are manifest as measurable seismic signatures. For example, receiver function and controlled source seismic studies provide detailed constraints on the depth of velocity discontinuities such as the Moho, the lithosphere–asthenosphere boundary and the mantle transition zone. Seismic velocities measurable using body and surface-wave tomography are strongly influenced by variations in mantle temperature and density. The alignment of olivine crystals in the flowing mantle results in seismic anisotropy, which can be quantified via analysis of shear-wave splitting and surface-wave studies of the directional dependence of seismic velocities. Many studies on the African continent in the last 20 years have per-formed these analyses and thus provide valuable constraints for the geodynamic community. It is the goal of this manuscript to review the seismologi-cal experiments that have been performed in Africa to date, with a view to understanding better the vari-able topography of the continent.

Following the approach of Burke (1996), discus-sion will be focused on three areas: southern Africa; east Africa; and central, north and western Africa. An overview of the topographic features and a brief discussion of the plausible tectonics and geo-dynamics is initially presented. We then review the recent regional seismic studies, focusing on crustal thickness, mantle velocity structure and observations of seismic anisotropy. Finally, we con-sider whether these studies provide direct evidence of the processes causing topographic variation and, in particular, how the seismic results may provide additional constraints for the ongoing geo-dynamical modelling. It is clear that there is no single factor controlling the topographic expression of the African continent.

African topography

Eastern Africa

Nyblade & Robinson (1994) proposed that southern Africa, the East African Plateau and part of the south-eastern Atlantic form a contiguous region: the African superswell. Comparisons of bathymetry and elevation with models of plate cooling and the global mean elevation of 565 m, respectively, shows that the African superwell has *c.* 500 m residual topography (Nyblade & Robinson 1994). Within east Africa there appear, however, two quite distinct regions with higher elevations: the Kenya/Tanzania dome and the Ethiopian Plateau (Ebinger *et al.* 1989). The topography of Kenya and Tanzania appears to be contiguous with the higher elevations throughout the south of the conti-nent, although its appearance is accentuated by the low-lying Congo Basin to the west (Fig. 1). In con-trast, the Ethiopian Plateau is clearly separated from

this area by a distinct NW–SE-trending topographic low (the Turkana Depression). On top of these broad swells, the scars of the EARS can also be seen. In the north, the Afar depression marks the region of the rift–rift–rift triple junction where the Red Sea and Gulf of Aden spreading centres meet with the EAR. The rift-related topography can be followed through Ethiopia, and then into the two branches surrounding the Archaean Tanzania Craton (Fig. 1).

Many authors have invoked thermal plumes to explain Africa's hotspot tectonism and uplift, but the location and number of plumes or upper mantle convective cells is often debated. For example, Ebinger & Sleep (1998) suggested that one large plume spread beneath the African Plate near Turkana at *c.* 45 Ma, but only small amounts of melt volume were produced until lithospheric thinning commenced in the Red Sea and Gulf of Aden rifts. Topography at the base of the lithosphere channelled buoyant material up to *c.* 1000 km from Turkana to the evolving Red Sea rift and the Mesozoic rift zones of eastern and central Africa. Alternatively, two Cenozoic plumes may have existed beneath East Africa, one rising and dispersing beneath southern Ethiopia at *c.* 45 Ma and the other rising beneath the Afar depression (e.g. George *et al.* 1998). More recent geochemical studies have explained their observations based on a modified single-plume hypothesis: multiple upwellings from the African superplume (Kieffer *et al.* 2004; Furman *et al.* 2006).

The timing of Ethiopia's high topography is perhaps somewhat better constrained than that of southern Africa due to the dating of the volcanism in the region. A thick pile (500–2000 m) of continental flood basalts and rhyolites were emplaced in the central Ethiopian Plateau *c.* 30 Ma (Hofmann *et al.* 1997; Ayalew *et al.* 2002; Coulie *et al.* 2003). This is thought to have been due to the impact of the Afar mantle plume, which was coeval with marked uplift of the plateau (*c.* 20–30 Ma; Pik *et al.* 2003). Isolated shield volcanism in the period *c.* 30–10 Ma occurred across the Ethiopian Plateau (Fig. 1) and added *c.* 2 km of additional local relief (e.g. Coulie *et al.* 2003; Kieffer *et al.* 2004). The temporal evolution of rift-related topography remains somewhat controversial. In southern Ethiopia, results from low-temperature (U–Th)/He thermochronometry suggest that the rift development has been continuous since initiation in the Miocene (Pik *et al.* 2008). In contrast, Gani *et al.* (2007) suggest that significant recent (*c.* 10 Ma) uplift was due to foundering of the Plateau lithosphere following extensive heating and weakening since the onset of flood basalt volcanism at *c.* 30 Ma.

Timing of plateau formation around Kenya and Tanzania is less well constrained. The earliest volcanism in Kenya started in the Turkana region of northern Kenya at *c.* 35–40 Ma (e.g. Furman *et al.* 2006), and has also been associated with the impingement of a mantle plume (e.g. George *et al.* 1998). Following the rift system to the south through Kenya and Tanzania, the onset of Cenozoic volcanism becomes progressively younger (e.g. Morley *et al.* 1992). Locally, there is also evidence for Neogene uplift along the flanks of some rift valleys (e.g. Spiegel *et al.* 2007).

Southern Africa

Within this broad area of uplifted topography (Fig. 1) there are regions with significant local variations. For example, significant topography is observed along much of the continental margin and has been associated with the break-up of Gondwana (*c.* 130 Ma). Although this relationship is questioned by Burke (1996), both voluminous sediment accumulation offshore of the southern coast (Tinker *et al.* 2008) and apatite–fission track studies (e.g. Brown *et al.* 2002) support a hypothesis of uplift and erosion at this time. However, recent analyses of river profiles on each of the southern African subswells (Bie, Namibia, Drakensburg; Fig. 1) indicates more recent (<30 Ma) uplift. Both the Bie Dome and the Drakensburg Escarpment show significant (0.5–1 km) uplift since *c.* 10 Ma, while the river profiles on the Namibian swell have been modelled successfully by continued uplift since the Oligocene (30 Ma; Roberts & White 2010). More recent post-Pliocene uplift has also been inferred on the Angolan margin from the analysis of offshore seismic data (e.g. Al-Hajri *et al.* 2009).

The cause of the elevated topography in southern Africa is less clear than in east Africa, where models involving mantle plumes have been invoked to explain volcanism that correlates spatially with the observed domal features. Geodynamic modelling from global tomographic models suggest that in southern Africa much of the elevation could be explained by density anomalies below 1000 km depth (e.g. Lithgow-Bertelloni & Silver 1999). Gurnis *et al.* (2000) noted that if the continental lithosphere is thick and has a high effective viscosity, an increased coupling between the deep mantle and surface can lead to increased elevations. Nyblade & Sleep (2003) proposed an alternative mechanism for supporting the high topography, suggesting that the combined effects of multiple plumes in the Mesozoic could generate sufficient long-lasting uplift to account for the present elevations.

Northern, central and western Africa

The remaining portion of Africa covers a wide region from the Congo Basin and Cameroon

Volcanic Line (CVL) in central Africa, across much of the Sahara and into the Atlas Mountains in the north (Fig. 1). At the northern margin of the continent, the high relief of the Atlas Mountains has been associated with the convergence of Africa and Europe (e.g. Frizon de Lamotte *et al.* 2000). Although the tectonic shortening appears to be relatively modest (e.g. Teixell *et al.* 2003), Buiter *et al.* (2009) show that significant topography can be reached through the inversion of a failed rift. Additionally, recent modelling of the lithospheric structure beneath the Atlas, using a variety of geoid, gravity, topography and heat-flow data, suggests that a NE–SW-trending strip of thinned lithosphere underlies the region (e.g. Zeyen *et al.* 2005; Fullea *et al.* 2007). A variety of geodynamical models have thus been proposed for this region: one suggestion being that a shallow mantle upwelling (Teixell *et al.* 2005) contributes to the regional topography.

The topographic swells in the central part of north Africa (e.g. Hoggar, Tibesti; see Fig. 1) have associated volcanism dating from the Oligocene (*c.* 30 Ma) through to the Quaternary (e.g. Wilson & Guiraud 1992). The volcanism has been related to the time period when the African plate became relatively stationary to mantle circulation and the distribution was explained by regions of fertile lithospheric mantle (e.g. Ashwal & Burke 1989; Burke 1996). Ebinger & Sleep (1998) showed that while channelling along regions of thin lithosphere would lead flow of plume material beneath the Darfur swell and towards the CVL, it could not explain the volcanism of Hoggar and Tibesti. Similarly, geochemical data also suggest very different characteristics between the volcanism in Hoggar and that found near the Afar hotspot (Pik *et al.* 2006).

In addition to the volcanic swells in northern Africa are a number of intracontinental basins (e.g. Taoudeni, Ghadames, Sirte and Al-Kufrah). The mechanisms for the subsidence of these and, indeed, all intracontinental basins remain heavily debated. Low strain-rate stretching (e.g. Armitage & Allen 2010), cooling of the lithosphere (e.g. Kaminski & Jaupart 2000) and dynamic subsidence (e.g. Heine *et al.* 2008) have all been proposed to explain the general behaviour of this style of basin. For northern Africa, Holt *et al.* (2010) recently illustrated that models of lithospheric cooling (from an originally thin lithosphere) can explain the subsidence history of the Ghadames and Al-Kufrah basins. There are, however, significant differences in estimates of the present-day lithospheric thickness beneath all the north African basins (see Priestley *et al.* 2008; Pasyanos 2010; Global and continental studies). For example, the Taoudeni Basin sits atop the thick lithosphere of the West African Craton, thus

indicating that varied mechanisms may be required for the different basins.

Further to the south, another intracontinental basin (the Congo Basin) provides the most noticeable region of low topography on the African continent (Fig. 1). Flanked by the CVL, Kenyan Dome and Bie Dome, the Congo Basin has accumulated 4–9 km of sediments beginning with extension in the Late Precambrian time and with subsidence continuing until the present day (see e.g. Daly *et al.* 1992; Giresse 2005). The long sedimentary history, in contrast to other extensional basins such as the North Sea, is difficult to explain and has important implications for the low topography observed today. Hartley & Allen (1994) suggested recent subsidence may relate to convective downwelling beneath the region, a hypothesis supported in the recent geodynamic modelling of Forte *et al.* (2010). Analysis of geophysical data over the basin has given varied results. From analysis of the gravity signature, Downey & Gurnis (2009) inferred a high-density anomaly within the mantle lithosphere. In contrast, the modelling of Crosby *et al.* (2010) suggested that the extended period of subsidence could be explained by extension and subsequent cooling of initially thick lithosphere, and interpreted the gravity anomaly in terms of recent convective drawdown.

Passive seismic experiments in Africa

Our understanding of the structure of the crust and upper mantle beneath Africa has advanced significantly over the last 15 years, primarily due to the deployment of broadband seismometers either as permanent stations or as temporary networks designed to investigate specific geological and tectonic problems. Over the last 20 years, networks such as Geoscope, Geofon, US Geological Survey (USGS), Incorporated Research Institutions for Seismology/ International Deployment of Accelerometers, IRIS/ USGS and the Mediterranean Broadband Seismographic Network have provided publicly available broadband data from permanent stations in many countries, including: Algeria, Botswana, Central African Republic, Djibouti, Egypt, Ethiopia, Gabon, Ivory Coast, Kenya, Madagascar, Mali, Morocco, Namibia, Senegal, South Africa, Tunisia, Uganda and Zambia (Fig. 2).

In addition to the data available from the global networks, the ongoing AfricaArray project (Nyblade *et al.* 2008) is rapidly increasing the number of permanent broadband seismometers within the African continent (Fig. 2). Supplementing the permanent networks, a number of large active and passive land-based regional experiments have been carried out and significantly increase the
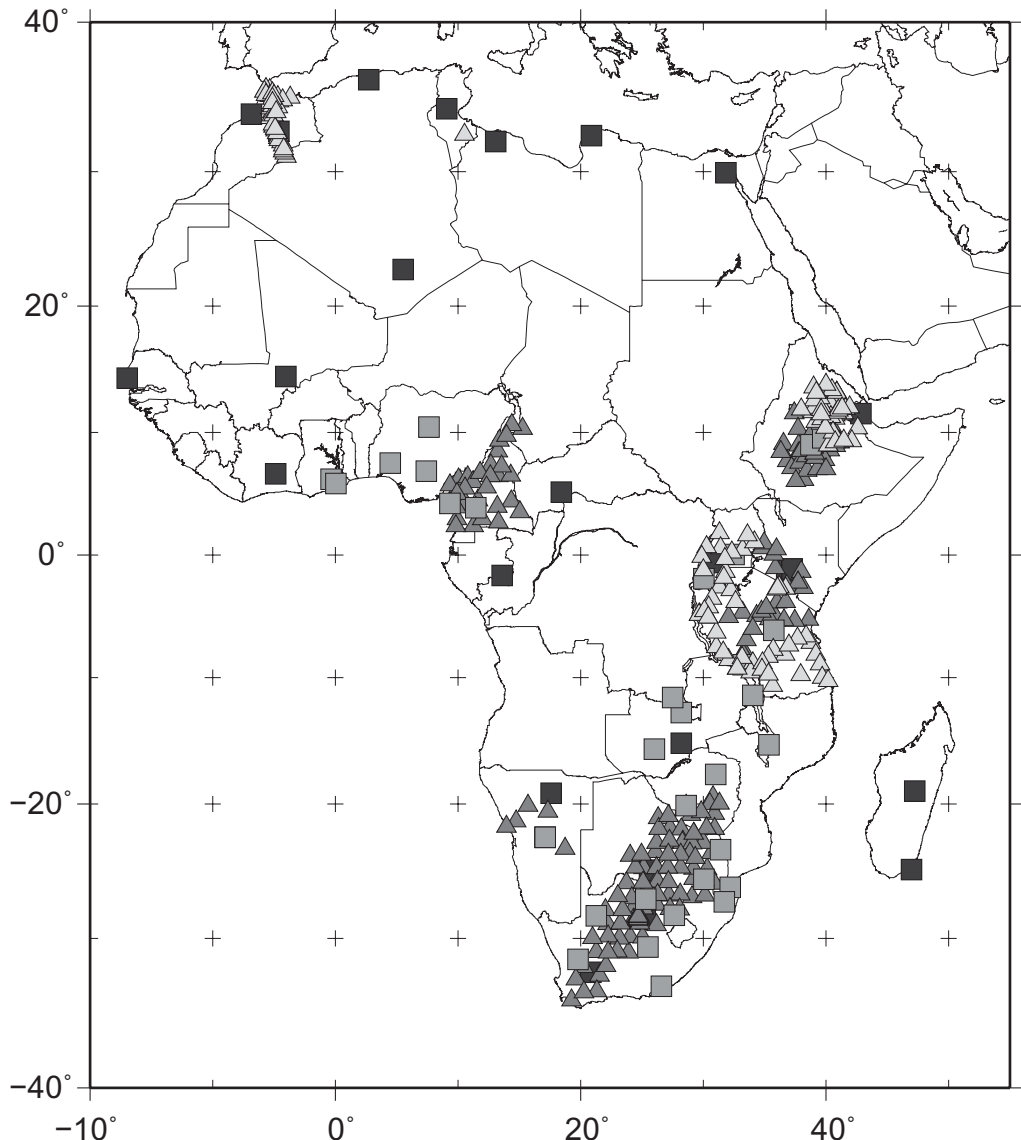
Fig. 2. Map of broadband seismic stations (1990–2010) with data available through IRIS-Data Management Centre or Geofon-GFZ Potsdam. Black squares show permanent seismograph stations from global networks; grey squares show stations as part of Africa Array (Nyblade *et al.* 2008); dark grey triangles show stations from temporary networks operating between 1995–2008 (e.g. Carlson *et al.* 1996; Nyblade *et al.* 1996; Hanka *et al.* 2000; Nyblade & Langston 2002; Maguire *et al.* 2003; Tibi *et al.* 2005; Wölbern *et al.* 2010); light grey triangles show temporary networks operating from 2008 to present.

available data (Fig. 2). The purpose of Africa's portable seismic experiments has been broad-ranging. In east Africa, the principal goal has been to understand hotspot tectonism and the development of various stages of rifting from embryonic continental rifting in the south to incipient sea-floor spreading in Afar (e.g. Nyblade & Langston 2002; Maguire *et al.*

2003). The Precambrian cratons of Tanzania and southern Africa have also been studied seismically, with the goal of understanding the processes that shaped the early Earth (e.g. Carlson *et al.* 1996; Nyblade *et al.* 1996). In Cameroon, seismic data have been collected in order to investigate the origins of the CVL (Tibi *et al.* 2005) which,

unusually for an intra-plate volcanic line, has no age progression and has been attributed variously to plume flow and small-scale convection models. Each of these tectonic and geodynamic processes have seismological signatures with important implications for the development of topography. Further projects have either recently begun (e.g. Morocco) or are scheduled to begin soon (e.g. Zambia, Mozambique, Morocco), so the African seismic database will continue to grow in the coming years.

Review of seismological observations

In the following sections we follow the approach of Burke (1996) by summarizing seismological constraints from three areas: east Africa, southern Africa and central/north/west Africa. In doing so, we focus on the seismological results that have first-order importance for understanding topography. We first consider variations in crustal thickness, which have significant implications for isostasy. Mantle seismic velocity structure is then reviewed in the light of the causes and support of topography. Finally, because of its potential to place constraints on the mantle flow field beneath the continent, we summarize constraints from studies of mantle anisotropy.

Estimates of crustal thickness

Global and continental studies. Many geodynamic studies of the African continent proceed on the assumption that the crust can be adequately described by global models such as 3SMAC (Nataf & Ricard 1996) or Crust 2.0 (Bassin *et al.* 2000; Fig. 3a, b). These models are however relatively simple and lack the fine-scale details revealed by regional seismic experiments. 3SMAC, for example, is defined by only three layers: sediments and upper and lower crust. Thicknesses of the layers are constrained from a variety of geophysical compilations, inherently having non-uniform coverage (Nataf & Ricard 1996). In contrast, Crust 2.0 is more complex with five layers to allow for variable sediments, and an additional middle crustal layer (Bassin *et al.* 2000). Each point on the 2×2 degree grid is given a key 1D profile to assign various types of crustal structure. The velocities and densities are then dependent on the type of crustal structure; these key profiles and associated density variations are thus important when estimating crustal isostasy.

Although lacking the resolution of local studies, short-period surface-wave studies using broadband seismic stations deployed across the African continent provide an improved spatial resolution compared to the global crustal models. Using an analysis of group velocity dispersion, Pasyanos & Nyblade (2007) present a crustal thickness map for the African continent (Fig. 3c) as well as estimates of crustal and mantle velocities. Although the path coverage is uneven, at short periods the uncertainties on the group velocity measurements should be small; uncertainties in crustal thickness will be due principally to the model parameterization and the trade-off between crustal thickness and velocity.

In contrast to the global models, a thinner crust (*c.* 30 km) is observed beneath much of northern
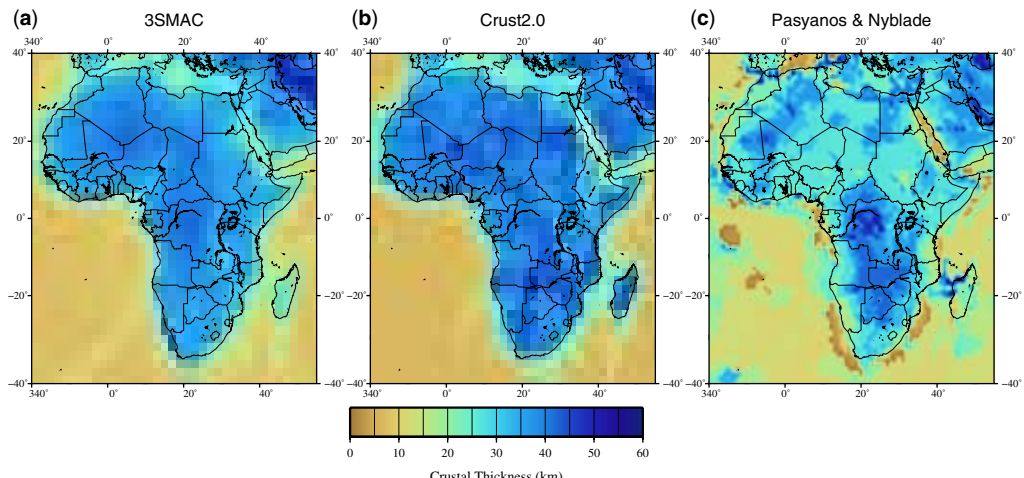
**Fig. 3.** Crustal thickness variation across Africa. Estimates taken from: (**a**) the global model 3SMAC (Nataf & Ricard 1996); (**b**) the global model Crust2.0 (Bassin *et al.* 2000); and (**c**) the surface-wave study of Pasyanos & Nyblade (2007).

Africa and a thicker crust (*c.* 40 km) is seen beneath many of the cratonic keels of the African land mass (Kaapvaal, Congo, West African Craton; Fig. 3). The general increase in crustal thickness in the south of the continent is consistent with the higher elevations observed in the region. However, perhaps surprisingly given their low elevation, the thickest crust in the cratonic regions is observed beneath the Congo Basin (*c.* 45–50 km) and the Taudeni Basin (*c.* 40–45 km) in NW Africa. Other features absent from the global crustal models but identified in the Pasyanos & Nyblade (2007) study include the thinner crust between the Ethiopian and East African plateaus, and thin crust beneath the Benue Trough in west Africa (Fig. 3c).

Eastern Africa. East Africa has been host to some of the largest seismic experiments in the world whose focus has been the improved understanding of the transition from embryonic continental rifting in the south to incipient sea-floor spreading in Afar (e.g. Maguire *et al.* 2003; Bastow *et al.* 2011). Although detailed constraints on crustal structure come from wide-angle profiles in select parts of the EAR system (e.g. KRISP Working Group 1987; Prodehl & Mechie 1991; Maguire *et al.* 2006), the best spatial coverage of crustal thickness comes from analysis of P-to-S converted phases from the Moho captured during receiver function analysis. A common approach is the so-called H–K stacking procedure of Zhu & Kanamori (2000), which uses P-to-S converted phases from teleseismic earthquakes to constrain bulk-crustal properties (crustal thickness and VpVs ratio) beneath a seismograph station.

In Ethiopia, receiver function studies (Dugda *et al.* 2005; Stuart *et al.* 2006; Cornwell *et al.* 2010) corroborate the wide-angle results (Mackenzie *et al.* 2005; Maguire *et al.* 2006), indicating that extension in the Ethiopian rift is achieved without the marked crustal thinning that would be predicted from many traditional models of break-up. Moho depths are *c.* 40 km on the Ethiopian and Somalian plates, and 32–36 km within the rift (Fig. 4b). These observations, coupled with evidence of crustal melt zones imaged by magnetotelluric study (Whaler & Hautot 2006) and the spatial coincidence of seismicity in and around the rift associated with these zones of partial melt (Keir *et al.* 2009), indicate that extension is accommodated principally by magma intrusion into the extending plate. Only further north in Afar does the crust appreciably thin to *c.* 25 km (Dugda *et al.* 2005), coincident with a marked reduction in elevation towards and ultimately (in the Danakil Depression) below sea level.

Further south adjacent to the Kenya rift, receiver functions suggest a crustal thickness of 39–42 km to the east of the rift and *c.* 38 km to the west (Dugda *et al.* 2005). While there is little information from passive seismic studies on the crustal thickness along the rift itself, analysis of seismic refraction and wide-angle reflection data from the Kenya Rift International Seismic Project (KRISP) experiments suggest that the crustal thickness varies from 35 km in the south beneath the Kenyan dome to as little as 20 km beneath the low-lying Turkana depression (Mechie *et al.* 1997). Regional Rayleigh wave dispersion data (Benoit *et al.* 2006*b*) and the continent-wide study of Pasyanos & Nyblade (2007) corroborate these controlled source results and show that Mesozoic crustal thinning can explain the low-elevation region that separates the Ethiopian and East African plateaus.

Beneath the western branch of the rift system, recent analysis of teleseismic data has suggested crustal thickness of *c.* 30 km on the rift shoulder and significantly thinner crust (*c.* 20–28 km) beneath the Rwenzori block, where the mountains reach elevations of more than 5000 m (Wölbern *et al.* 2010; Fig. 4d). These recent observations of thin crust beneath regions of very high elevation are in marked contrast to normal Airy isostasy, suggesting that alternative mechanisms such as delamination of a lithospheric block may have caused the uplift (Wölbern *et al.* 2010). Further to the SE below the cratonic region of Tanzania, crustal thickness estimates are *c.* 40 km with slightly thicker crust beneath the Ubendian Belt on the SW margin of the craton (Last *et al.* 1997; Julià *et al.* 2005; Fig. 4d).

Southern Africa. Within southern Africa a number of studies have used receiver functions to determine the crustal structure (e.g. Nguuri *et al.* 2001; Niu & James 2002; Stankiewicz *et al.* 2002; Nair *et al.* 2006). These studies have been in broad agreement and show crust of *c.* 38 km beneath much of the Kaapvaal Craton, with the exception of a *c.* 44 km thick region adjacent to the Limpopo Belt (see Appendix A). Further to the south, the Namaqua Natal Mobile Belt and Cape Fold Belt is underlain by variable, thick crust (*c.* 36–50 km), and there is significantly thinner crust (*c.* 26 km) on the oceanic side of the escarpment at the very southwestern margin of the continent (see also Harvey *et al.* 2001). One of the most recent studies of the crust beneath the Southern Africa Seismic Experiment (SASE) array (Kgaswane *et al.* 2009) also incorporates group-velocity surface-wave data from Pasyanos & Nyblade (2007) and Larson & Ekström (2001) alongside the receiver functions, and finds similar estimates of Moho depth (see Fig. 4c) beneath the cratonic region. However, beneath the Namaqua Natal Mobile Belt, the results from the joint inversion generally suggest
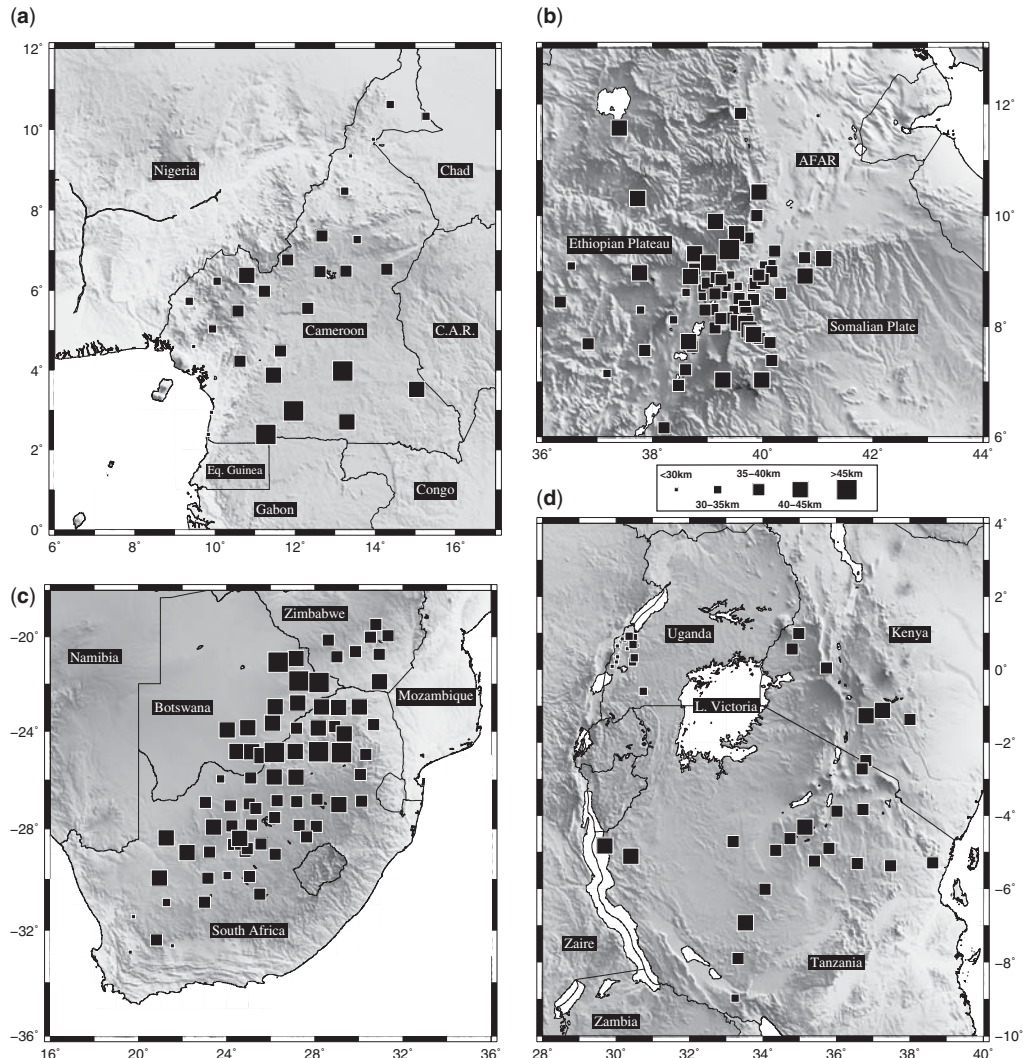
Fig. 4. Crustal thickness constraints for the African continent constrained using receiver function analysis. Data are sourced from (**a**) West Africa – Tokam *et al.* (2010); (**b**) Ethiopia – Dugda *et al.* (2005); Stuart *et al.* (2006); highest signal-to-noise ratio crustal constraints from the study of Cornwell *et al.* (2010) are also used; (**c**) Southern Africa – Kgaswane *et al.* (2009); (**d**) Eastern Africa – Last *et al.* (1997); Dugda *et al.* (2005); and Wölbern *et al.* (2010). CAR, Central African Republic. Station locations and crustal thicknesses are listed in Appendix A.

thinner crust than indicated by the receiver functions alone (Fig. 4c; Appendix A).

Further constraints on crustal thickness come from the ambient noise tomography of Yang *et al.* (2008), with additional information from the teleseismic two-plane-wave tomography study of Li & Burke (2006). Encouragingly, beneath much of the cratonic region the results are in good agreement with the study of Nair *et al.* (2006) and Kgaswane *et al.* (2009), indicating thickened crust through the northern Kaapvaal Craton and Limpopo Belt.

Because the results from different seismic techniques show good agreement, the confidence in the crustal thickness estimates is enhanced. It is noticeable, however, that the abrupt changes in crustal thickness within the Kaapvaal Craton are not always mirrored by topographic variations expected from simple Airy isostasy (Nair *et al.* 2006; Yang *et al.* 2008). This observation has been confirmed by modelling of the Bouguer gravity anomaly over the Bushveld complex, where high-density mafic rocks are required to

provide the mass within the crustal section to balance the thickened root (Webb *et al.* 2004).

Northern, central and western Africa. Seber *et al.* (2001) developed a 3D crustal model for the middle-east and north Africa, combining data from crustal-scale refraction and reflection profiles, receiver functions, gravity modelling and surface-wave data. The limited seismic data through much of north Africa means that this model is predominately based on inferences from the geology of the region with significant interpolation between few data points. The results indicated thickest crust (>40 km) towards the SW margin of the West African Craton (Seber *et al.* 2001). Elsewhere in northern Africa, detailed knowledge is absent due to the lack of data. However, the recent study by Liu & Gao (2010) analysed the crustal structure beneath the GEOSCOPE seismograph station at Tamnarasset, immediately adjacent to the Hoggar swell. Almost 20 years of data were available for the station, leading to an exceptionally high-resolution study. Crustal thickness is observed to be *c.* 34 km, although there is significant contrast in the observed receiver functions between adjacent geological terranes (Liu & Gao 2010). There is no obvious increase in crustal thickness detected by raypaths that have Moho conversions close to the Hoggar swell. However, the lack of seismic stations deployed directly on the swell precludes any unambiguous testing of isostatic crustal thickness variations.

In western Africa, the recent seismic experiment investigating the CVL provides detailed information on crustal thickness. Using a joint inversion of receiver functions with Rayleigh wave-group velocities, Tokam *et al.* (2010) find significant variation in Moho depths (Fig. 4a). Beneath the CVL the Moho is observed at 35–39 km depth, similar to the depths observed in the adjacent Pan-African belt. Thicker crust is observed under the margin of the Congo Craton (*c.* 43–48 km), associated with the continent–continent collision during the formation of Gondwana; thinner crust to the north (*c.* 26–31 km) is likely to be related to the formation of the Benue Trough (Tokam *et al.* 2010). These recent estimates of crustal thickness from receiver functions are also in agreement with earlier seismic refraction studies (Stuart *et al.* 1985). Across the CVL there is also a good correlation between the crustal thickness estimates and the Bouguer gravity anomaly (Tokam *et al.* 2010).

While topographic variations on the African continent are often mirrored by isostatically predictable variations in crustal thickness (e.g. thinned crust beneath the rifts of western and eastern Africa), the lack of correlation between elevation and Moho depth in other areas implies that other mechanisms must be contributing to the observed topography. In the following section we review

present-day understanding of Africa's mantle seismic structure in an effort to examine the role of the mantle in controlling topography.

Velocity variations in the upper mantle

While seismic velocities are affected by factors such as melt, water, composition and grain size, within the upper mantle temperature is generally considered the dominant control on velocity (e.g. Goes *et al.* 2000; Faul & Jackson 2005). Studies that provide information on the lateral and vertical variation in seismic velocity are therefore crucial in providing information on likely temperature variations. In turn, knowledge of mantle velocity structure helps determine mantle contributions to the development and maintenance of topography. The structure of the mantle transition zone (MTZ) is also sensitive to variations in temperature. The opposite Clapeyron slopes of the 410 and 660 km discontinuities should lead to a thickened MTZ in cold regions and a thinned MTZ in hot regions (Bina & Helffrich 1994). The depth of the discontinuities can be determined, for example, by receiver function analysis, adding seismological constraints on thermal structure to those derived from the tomographic studies.

Global and continental studies. The deep seismic structure of Africa is presented by numerous global tomographic inversions using data from the global seismic networks (e.g. Grand 2002; Ritsema & Allen 2003; Montelli *et al.* 2006; Li *et al.* 2008; Simmons *et al.* 2010). One dominant feature common to all models is the African Superplume, a broad (*c.* 500 km wide), *c.* 3% S-wave slow-velocity anomaly that originates at the core–mantle boundary beneath southern Africa, and rises towards the base of the lithosphere somewhere in the region of Ethiopia and the Red Sea/Gulf of Aden. These global models, and the influence of the African Superplume, have been the focus of much of the geodynamic modelling beneath Africa and the adjacent regions (e.g. Lithgow-Bertelloni & Silver 1999; Gurnis *et al.* 2000; Daradich *et al.* 2003; Simmons *et al.* 2007; Forte *et al.* 2010).

The majority of global studies provide lower-resolution images of upper mantle structure than regional studies. Body wave tomographic inversions generally require relatively close station spacing (≤200 km) in a region of interest to place accurate constraints on structure in the upper *c.* 300 km. Given the uneven distribution of seismic stations across Africa, surface-wave studies that constrain seismic structure along the great circle path between the source and the receiver are therefore a vital technique to image the velocity variations in the upper mantle on a continental-scale. Since the propagation of surface waves is

predominately within the crust and upper mantle (dependent on the frequency and mode of surface wave studied), it is therefore possible to achieve good path coverage and resolution in regions with no seismic stations (see e.g. Fishwick 2010), given a good distribution of seismic sources.

A number of global and regional surface-wave studies including Africa have been performed during the last fifteen years (e.g. Ritsema & van Heijst 2000; Debayle *et al.* 2001; Sebai *et al.* 2006; Pasyanos & Nyblade 2007; Lebedev & van der Hilst 2008; Priestley *et al.* 2008; Fishwick 2010). Within the upper mantle the dominant feature of these models is the contrast between the fast velocities associated with Precambrian lithosphere and much slower velocities (5–10%) beneath the rest of the continent. Figure 5 shows the results from the studies of Fishwick (2010) and Lebedev & van der Hilst (2008). While both studies use surface-wave data, different inversions codes and datasets (regional and global, respectively) are used. The similarity in results, which show the lateral extent of fast velocities and clearly highlight the different cratonic regions, is encouraging and suggests they are a reliable representation of the velocity structure. If these ancient cores, depicted by regions of fast velocity, have thermal anomalies that are completely balanced by compositional density differences (the isopycnal hypothesis proposed by Jordan 1975), there should be no residual topographic expression. In Africa, the cratonic regions of the NW and the south have contrasting topographic signatures, implying that the physical properties of the cratonic lithosphere are, indeed, not the principal cause of the broad-scale topographic variation.

A secondary geodynamic feature that may be associated with changes in lithospheric structure is upwelling caused by edge-driven convection (e.g. King & Anderson 1998). This process has been invoked as a possible cause for the intraplate volcanoes on the African continent (King & Ritsema 2000), and could therefore contribute to the observed topographic swells. In east Africa, seismic results show a clear link between melt, upper mantle slow velocities and slow velocities in the deep mantle (see below), indicating that the volcanism and high topography is not primarily caused by edge-driven convection. However, in other African regions the results are less clear. Montagner *et al.* (2007) suggest that many of the hotspots in northern Africa are only associated with shallow slow-velocity anomalies, compatible with an edge-driven origin. In SW Africa, Al-Hajri *et al.* (2009) associated the Bie Dome with slow-velocity anomalies in the upper mantle.

More recently, attempts have been made to quantify lithospheric thickness variations beneath parts of Africa from surface-wave results (e.g.

Priestley *et al.* 2008; Fishwick 2010; Pasyanos 2010). Figure 6 shows the lithospheric thickness estimates for the whole of Africa from the recent tomographic study of Fishwick (2010), which is broadly similar to that of Priestley *et al.* (2008) and Pasyanos (2010). For example, all the models show thick lithosphere (*c.* 200 km) beneath NW Africa, although whether or not this extends to the northern continental margin beneath the Atlas mountains remains ambiguous. Within central Africa, there remains significant debate as to the lateral extent of thick lithosphere (and fast seismic velocities) beneath the Congo Basin. It appears that the lithosphere thins towards the eastern margin of the basin; however, the thickness estimates differ significantly (*c.* 180 km – Fig. 6 and *c.* 120 km – Pasyanos 2010). Improved knowledge of lithospheric thickness and structure beneath the basin has important consequences in understanding the subsidence history and present-day topography of the region (Downey & Gurnis 2009; Crosby 2010; Forte 2010).

The filtered free-air gravity anomaly (e.g. GRACE data, Tapley *et al.* 2005) provides an additional source of information to make inferences on the cause of the topographic variation. Many regions with high topography (e.g. Atlas, Hoggar, Tibesti and Bie) correlate with positive gravity anomalies, are close to the edge of the regions of thick lithosphere and/or are underlain by thin lithosphere (Fig. 6). These results suggest that the surface expression of mantle upwelling may be controlled by the edge of the cratonic lithosphere. Without further geodynamical modelling however, it is not possible to say whether this is edge-driven convection (e.g. the model proposed by King & Ritsema 2000) or simply rapid changes in lithospheric structure influencing the larger-scale mantle flow field.

Eastern Africa. P- and S-wave tomographic images (Fig. 7) presented by Bastow *et al.* (2008) corroborate a growing body of evidence that Ethiopia is underlain by a broad (*c.* 500 km wide) low-velocity zone (Debayle *et al.* 2001; Grand 2002; Benoit *et al.* 2006a; Li *et al.* 2008; Simmons *et al.* 2009) that connects to the African Superplume in the lower mantle. There is no evidence for a narrow (*c.* 100–200 km diameter) plume tail beneath Ethiopia, as would be expected if a starting plume existed today. Absolute delay times at permanent station AAE in Addis Ababa, which indicate the mantle beneath Ethiopia is among the slowest worldwide (Poupinet 1979; Bastow *et al.* 2008), strongly suggest that high temperatures and partial melt are necessary to explain the seismic observations. The inference from these results is that it is reasonable to suggest that the upper mantle thermal anomaly is likely to have a significant role in the formation and support of the Ethiopian Plateau.
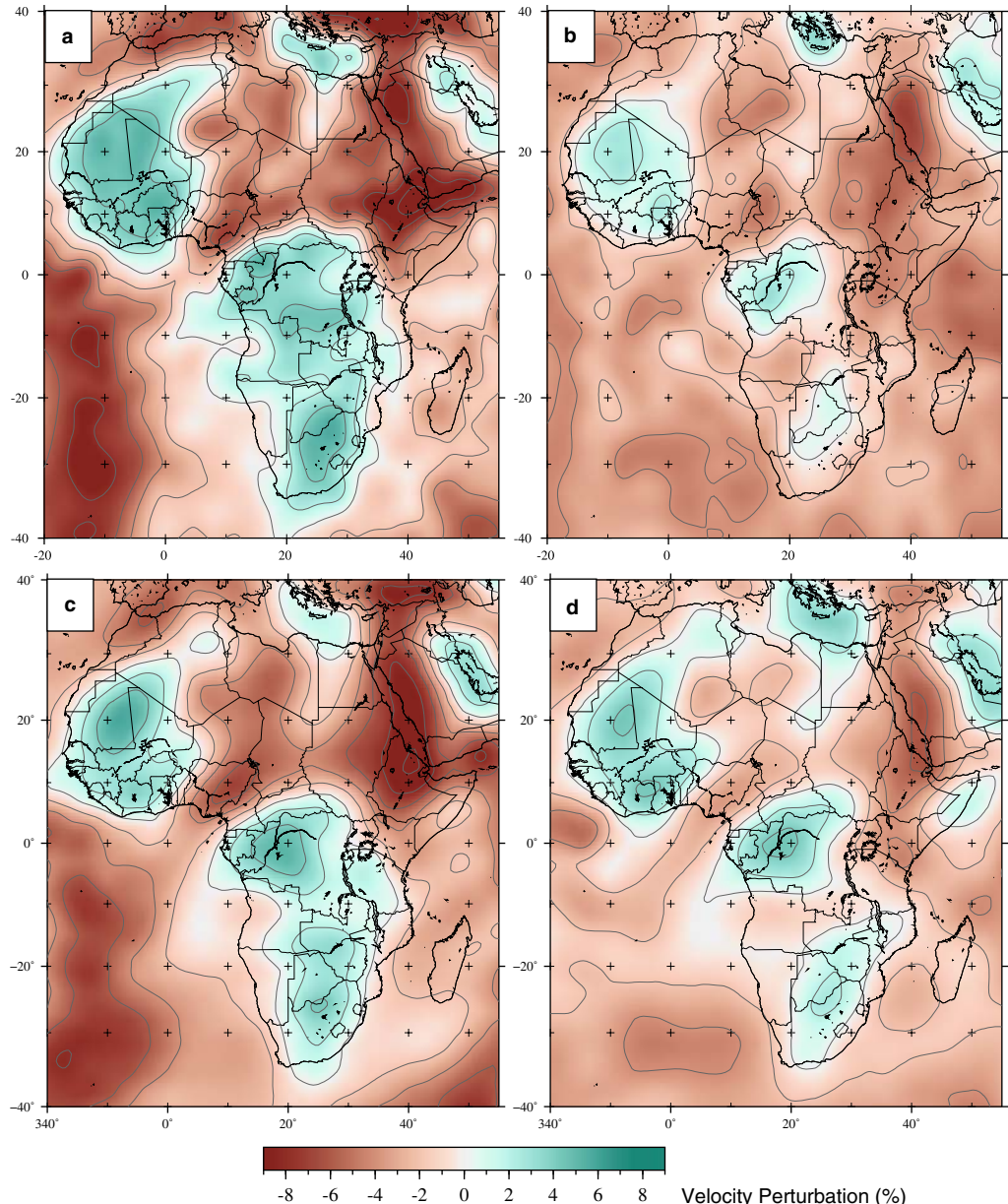
Fig. 5. Comparison of surface-wave models for the African continent. All data are plotted with the same colour scale and relative to the reference model ak135 (Kennett *et al.* 1995). Grey lines delineate 2% contour intervals in velocity perturbation. (**a**, **b**) Shear-wave speeds at 100 km and 200 km depth from the regional tomographic study of Fishwick (2010). (**c**, **d**) Shear-wave speeds at 110 km and 200 km depth extracted from the global tomographic study of Lebedev & van der Hilst (2008).

Further south in Kenya, low-velocity zones beneath the EAR are also imaged using body-wave seismic tomography (e.g. Achauer & Masson 2002; Park & Nyblade 2006). In Tanzania, tomographic images illuminate the *c.* 200–300 km deep high-

velocity lithosphere, which overlies low-velocity material that extends to at least 400 km depth (Ritsema *et al.* 1998). Surface-wave studies suggest a slightly thinner lithosphere than observed in other cratonic regions (e.g. Weeraratne *et al.*
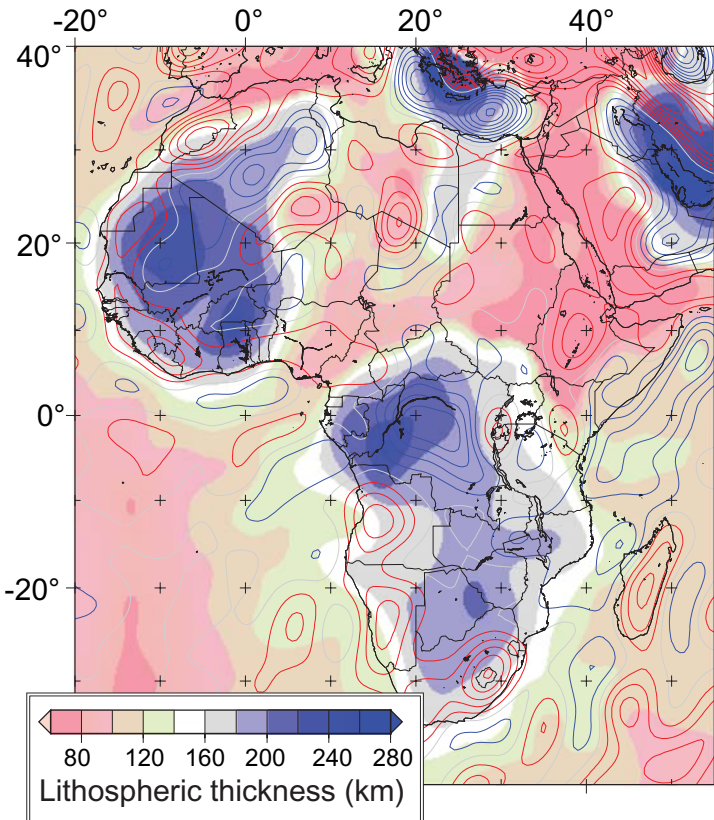
**Fig. 6.** Estimates of lithospheric thickness from the tomographic model of Fishwick (2010); velocities are converted to temperatures using the empirical parameterization of Priestley & McKenzie (2006). Red (positive) and blue (negative) contours show the long-wavelength free-air gravity anomalies from the GRACE data (Tapley *et al.* 2005).

2003; Fishwick 2010); shear velocities beneath the Tanzanian Craton are higher than a global average to a depth of 150 ± 20 km. Beneath Kenya and Tanzania there is significant variation in the depth of the 410 discontinuity, indicating potential variation in mantle temperatures at these depths; for large regions the estimated depth is $20-40$ km deeper than normal (Nyblade 2011).

The joint inversion of receiver functions and surface-wave dispersion data also suggests that there is significant difference in seismic velocities within the lithospheric mantle beneath Ethiopia and east Africa. The much slower velocities beneath Ethiopia suggest that this region has been affected to a much greater extent by a mantle thermal anomaly (e.g. Julià *et al.* 2005; Dugda *et al.* 2009). Given the similar domed topography seen in each region, the effects at lithospheric depths may be controlled by differences in the pre-existing lithospheric structure rather than significantly different thermal anomalies in the mantle

upwellings. A fundamental question that remains in east Africa is whether the Turkana Depression is low simply due to crustal isostasy (e.g. Benoit *et al.* 2006b) or whether there are also differences in mantle upwellings in the region.

Southern Africa. A significant focus of the work on southern Africa has been to obtain high-resolution models of the lithospheric structure beneath the Kaapvaal Craton. For example, array-based techniques using surface waves have been applied to map fine-scale variation in velocity structure (Li & Burke 2006; Chevrot & Zhao 2007). Detailed body-wave tomography has also been performed using the SASE data (James *et al.* 2001; Fouch *et al.* 2004), indicating the continuation of fast wave speeds (relative to an unknown background model) to depths of $300-400$ km (Fig. 7). All these models show heterogeneity within the upper mantle, but provide little conclusive evidence as to the possible cause of the elevated topography of southern Africa.
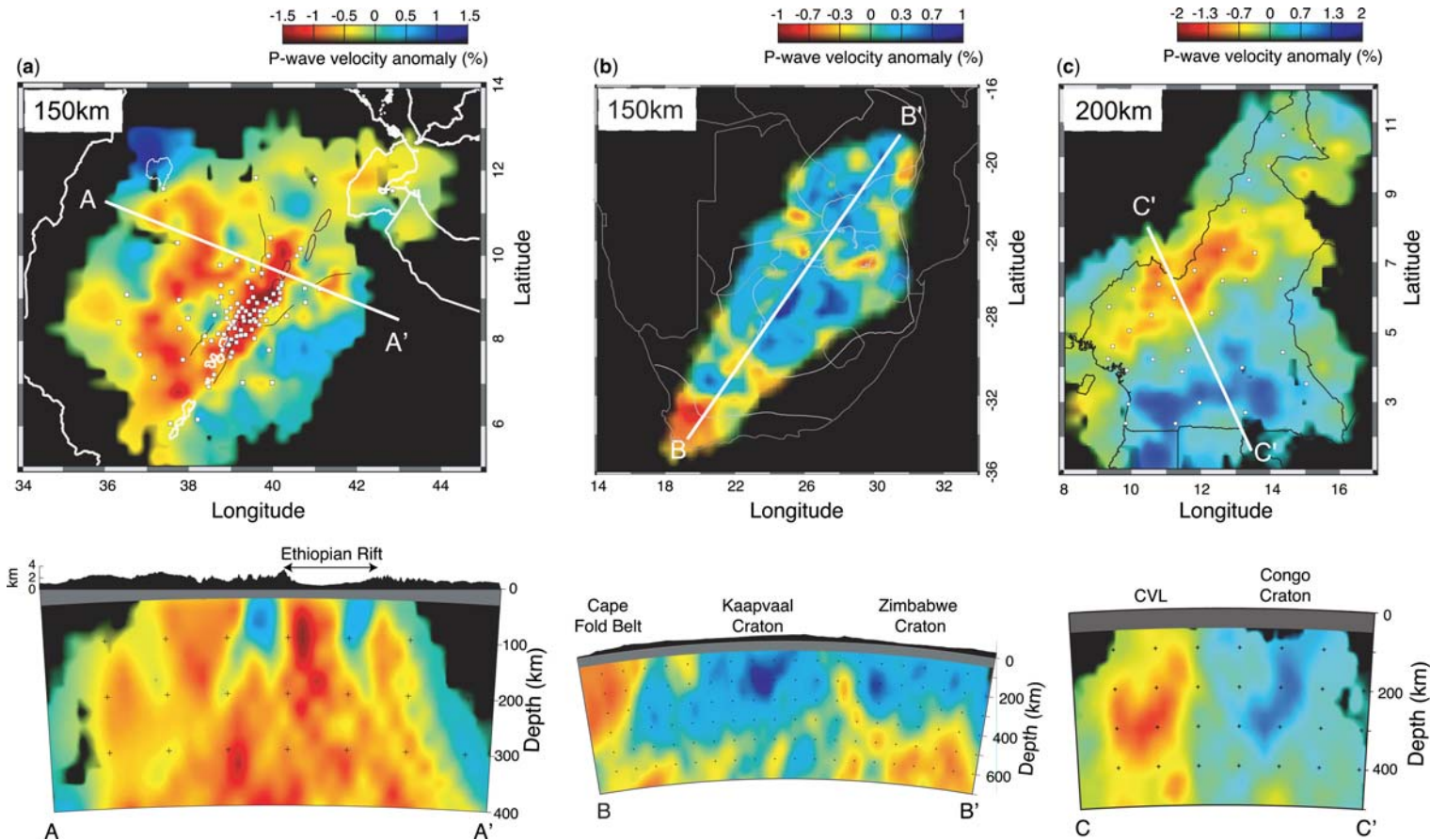
Fig. 7. Upper: Depth slice through the P-wave velocity model of (**a**) Bastow *et al.* (2008) from Ethiopia, (**b**) Fouch *et al.* (2004) from South Africa and (**c**) Reusch *et al.* (2010) from Cameroon. White squares are seismic station locations in (a) and (c). In (a) black lines in the depth slices show locations of Quaternary magmatic centres and Mid-Miocene border faults. Areas of low ray density are black. Lower: Cross-sections through each of the models (orientation of the cross-section is shown on the depth slice by a white line. The grey bands at the top of these preclude the view of shallow structure unresolved in the inversions. In each model, velocity structure is retrieved using regularized non-linear least-squares inversion of relative arrival-time residuals as described by VanDecar *et al.* (1995). The use of relative arrival-time residuals and not absolute delay times means that the zero anomaly level in each model is the background mean value of the region, which is not necessarily the global average.

However, one area of significant debate has been the existence of any upper mantle low-velocity zone beneath the Kaapvaal Craton. While the body-wave tomography suggests fast velocities to >300 km depth, modelling of triplicated body-wave phases suggests a distinct low-velocity zone beneath 150 km depth (Wang *et al.* 2008). Results from surface-wave analysis show similar discrepancies; some studies indicate a low-velocity zone is required to fit dispersion data (e.g. Priestley 1999; Pedersen *et al.* 2009); other studies show no indication of the low-velocity zone but instead have a change in anisotropy (Freybourger *et al.* 2001). Recently, Priestley & Tillmann (2009) have shown that the surface-wave tomography and body-wave tomography results are not necessarily incompatible, due to the difficulty of estimating the absolute velocity variation with depth for the body-wave models.

Imaging of mantle discontinuities using receiver functions has also indicated the existence of a low-velocity zone beneath southern Africa. A number of studies have placed the depth to this transition of *c.* 150 km (e.g. Savage & Silver 2008; Hansen *et al.* 2009*a*, *b*; Vinnik *et al.* 2009; Moorkamp *et al.* 2010). Whether this discontinuity is the lithosphere–asthenosphere boundary or is instead related to a change in physical properties within the subcontinental lithospheric mantle remains an area of debate (see e.g. Fishwick 2010; Rychert *et al.* 2010 for further discussion).

If the low-velocity zone beneath the Kaapvaal is caused by thermal anomalies and thus provides support to the high topography, then discontinuities within the MTZ may provide further indications of the depth extent of any anomaly and links to whole mantle convection. Using P- and S-receiver functions, Vinnik *et al.* (2009) suggest the presence of a distinct low-S-velocity layer above the 410 km discontinuity (also observed by Wittlinger & Farra 2007), high attenuation in the upper mantle and a discontinuity at 450 km depth. Although these features were attributed to the effects of plume-like phenomena in the upper mantle, there was no apparent thinning of the transition zone; the different arrival times from P660s and P410s phases were close to those from the IASP91 global reference model (Vinnik *et al.* 2009). Stankiewicz *et al.* (2002) also investigated the transition zone discontinuities for southern Africa. Beneath Kimberley the discontinuities were similar to the global average, while for other sections of the Kaapvaal Craton the 410 was slightly elevated and the 660 depressed (indicating a slightly cooler mantle temperature than normal; Stankiewicz *et al.* 2002). It therefore remains unclear as to whether there is any present-day thermal support for the high topography beneath southern Africa.

Northern, central and western Africa. The limited number of dense seismic networks makes it difficult to ascertain the extent of any anomalously high-temperature mantle underlying the volcanic swells in northern Africa. Hadiouche & Jobert (1988) indicated an east–west band of low velocities in the north of the continent; the slowest velocities were however observed further north than the Hoggar swell, beneath the Saharan basins and correlating to the location of high heat-flow measurements (Lesquer *et al.* 1990). Recent studies (e.g. Montagner *et al.* 2007; Priestley *et al.* 2008; Sicilia *et al.* 2008; Fishwick 2010) indicate low velocities within the upper mantle (Fig. 5), but do not provide a consistent view on either the exact location or depth extent. Due to the resolution limits of fundamental-mode-dominated surface-wave tomography, body-wave studies may eventually offer greater insight into the structure below 300 km depth; however, the lack of stations is presently a problem. Ayadi *et al.* (2000) showed slow upper mantle velocities beneath the Hoggar swell extending to depths of 300 km in some places. However, this was interpreted as modification of the lithospheric mantle rather than evidence of asthenospheric upwelling (Ayadi *et al.* 2000); the length of the profile also limits the maximum depth to where there is resolution. Studies using multiple-bounce body waves have the potential for good resolution in the upper mantle and have indicated slow wave speeds beneath Hoggar throughout the upper mantle (Begg *et al.* 2009) or, alternatively, very slow wave speeds in the transition zone (Simmons *et al.* 2009).

In western Africa, the velocity structure beneath the Cameroon Volcanic Line was investigated in the 1980s (Dorbath *et al.* 1986; Plomerová *et al.* 1993) and again in a recent seismic experiment (Reusch *et al.* 2010). All studies have shown low velocities in the uppermost mantle beneath the region (e.g. Fig. 7), although Dorbath *et al.* (1986) found no simple correlation with topography. Both Plomerová *et al.* (1993) and Reusch *et al.* (2010) attribute the velocity anomalies in the upper mantle to asthenospheric upwelling. The most recent results (Fig. 7) show a tabular low-velocity zone extending to at least 300 km depth which, when combined with the timing of volcanism in the region, corroborates the edge-driven convection hypothesis for the origins of volcanism in the region (Reusch *et al.* 2010). However, the depth extent of the low-velocity anomaly has yet to be resolved.

Seismic anisotropy

Seismic anisotropy (the directional dependence of seismic wave speed) can result from the alignment of minerals in the crust and mantle, the preferential alignment of fluid or melt or some combination

thereof (e.g. Blackman & Kendall 1997). This has the implication that studies of seismic anisotropy can place fundamental constraints on the present-day strain field that characterizes a tectonically active region; they are also capable of elucidating the strain field that acted in the past in regions now seismically and volcanically inactive (fossil anisotropy). Beneath the deforming plates the mantle flow field also imparts a seismic anisotropic fabric, principally due to the lattice preferred orientation (LPO) of anisotropic olivine crystals.

When a shear wave encounters an anisotropic medium, it splits into two orthogonal shear waves with one travelling faster than the other. Splitting can be quantified by the time delay (δt) between the two shear waves and the orientation (φ) of the fast shear wave (Silver & Chan 1991). Body-wave studies (e.g. Kendall et al. 2005) generally have good lateral resolution, but are limited to regions with seismic stations. In contrast, surface waves can be used to investigate seismic anisotropy along the great circle path between stations. Surface-wave particle motions decay with depth, dependent on their wavelength. Their velocity is therefore period dependent, a characteristic that can be exploited to resolve velocity as a function of depth. In tandem, therefore, combined study of body and surface waves can be used to place detailed constraints on strain and flow with depth (e.g. Bastow et al. 2010).

Geodynamic studies that predict mantle flow patterns (e.g. Forte et al. 2010) inherently make testable predictions about seismic anisotropy. For example, a vertically oriented olivine fabric resulting from a buoyant mantle plume would not be expected to produce significant shear-wave splitting in vertically propagating SKS phases. On the other hand, lateral flow of material along the lithosphere–asthenosphere boundary or aligned olivine at the base of a moving plate ('basal drag') are likely to be characterized by φ measurements parallel to the direction of flow (although complications do exist in the relationship between LPO and flow, e.g. Kaminski & Ribe 2002) and observations of large δt.

Global and continental studies. Given the number of proposed mantle upwellings beneath the African plate, the relatively slow horizontal plate motion and variations in lithospheric thickness, the mantle flow field at the lithosphere–asthenosphere boundary is likely to be particularly complicated. In a global model of azimuthal anisotropy, Debayle et al. (2005) indicate weak (<1%) anisotropy beneath much of central and southern Africa at depths of 200 km. Slightly larger values are observed towards the northern and eastern margin of the continent. Using the same inversion technique but on a continent scale, Priestley et al. (2008) also

found similarly low magnitudes of anisotropy at depths below 150 km. The low magnitude of azimuthal anisotropy suggests either weak horizontal flow or spatially variable anisotropy that shows no consistent direction when averaged over the spatial resolution of the surface-wave studies. However, using surface waves once more but applying a different methodology, Sebai et al. (2006) indicate that a general north–south trend in the fast direction of anisotropy is observed beneath the continent at depths of 200–300 km away from Afar.

The uncertainties in magnitude and direction of anisotropy beneath Africa in surface -ave studies means that comparisons of geodynamical models with seismic anisotropy have presently focused on results from shear-wave splitting analyses. Behn et al. (2004) compare shear-wave splitting measurements at thirteen ocean island stations surrounding Africa with varying geodynamic models. For stations away from mid-ocean ridges, the anisotropy was best explained by a model which incorporated large-scale upwelling originating in the lower mantle alongside plate motions (Behn et al. 2004). Forte et al. (2010) compare both flow direction and the horizontal component of maximum stretching from their geodynamic model with SKS results. While the relationship between either flow or stretching and the SKS results appears complicated, along the East African Rift there is a very strong subhorizontal flow field that likely also contributes to observed seismic anisotropy (Forte et al. 2010).

Eastern Africa. A number of workers have presented studies of SKS shear-wave splitting along the East African Rift System (e.g. Kendall et al. 2006; Fig. 8). In Tanzania and Kenya, fast polarization directions parallel the eastern and western branches of the rift system that surround the Tanzania Craton (e.g. Gao et al. 1997; Walker et al. 2004). The strength of seismic anisotropy is much lower in the south where the rift is least evolved. Measurements away from the rift, from the craton and the SE part of the EAR extending into the Mozambique Belt, are somewhat different however (Walker et al. 2004). Beneath the Tanzanian Craton, splitting is much weaker and oriented in a more east–west direction parallel to Precambrian structural trends (e.g. Shackleton 1986). Walker et al. (2004) interpret the splitting patterns in Tanzania in terms of a number of mechanisms including asthenospheric flow around a cratonic keel, plume–lithosphere interactions, pre-existing lithospheric fabric and melt-induced anisotropy.

Ayele et al. (2004) interpreted splitting measurements in Kenya, Ethiopia and Djibouti in terms of melt inclusions noting that the magnitude of splitting increases from the south to the north, consistent
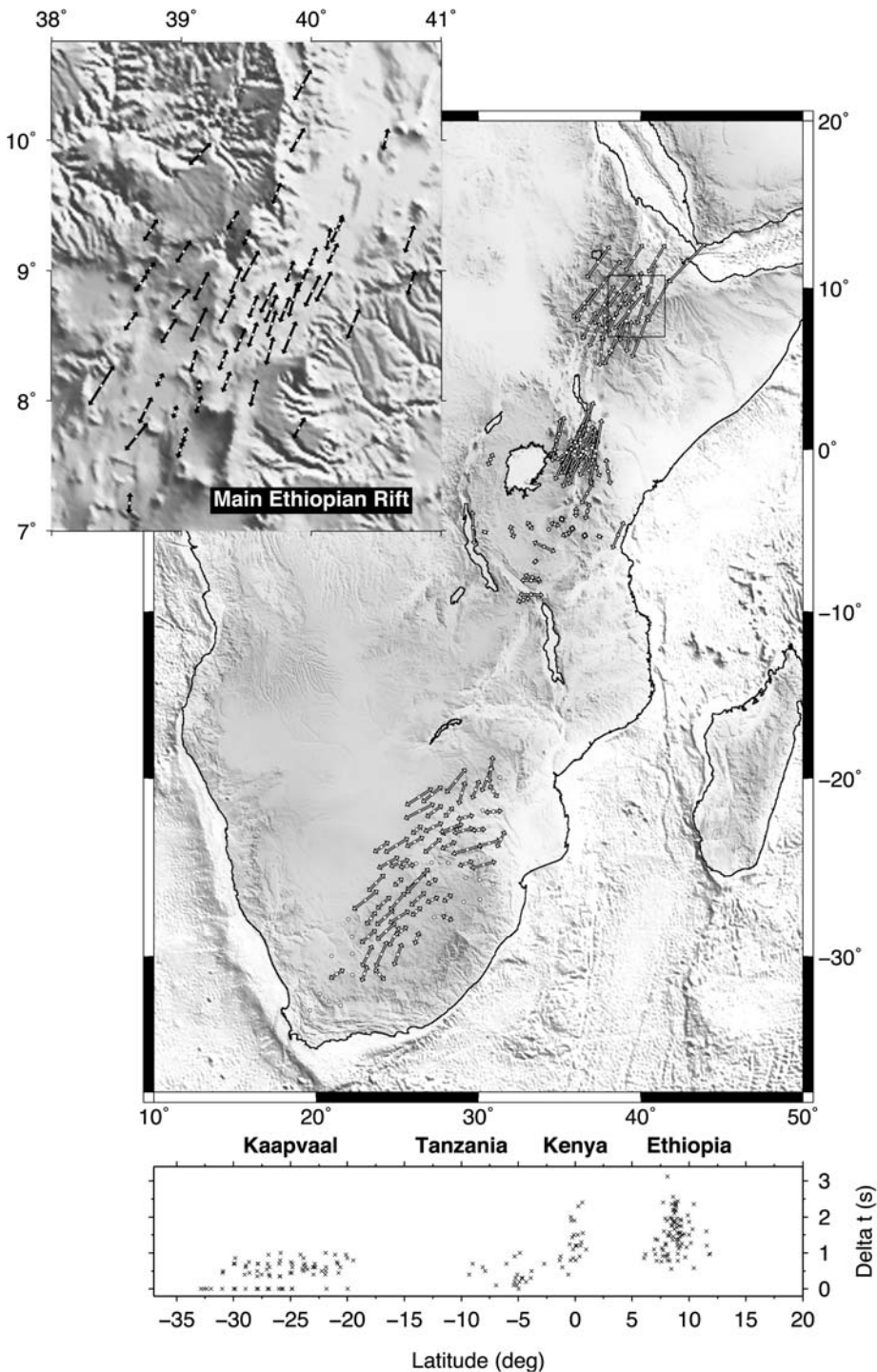
Fig. 8. Compilation of SKS shear-wave splitting measurements from the East African Rift (Gao *et al.* 1997; Ayele *et al.* 2004; Gashawbeza *et al.* 2004; Walker *et al.* 2004) and southern Africa (Silver *et al.* 2001). In the inset figure, detailed splitting observations from the Ethiopia Afar Geoscientific Lithospheric Experiment (EAGLE) experiment are from Kendall *et al.* (2005). In both maps, arrows show the orientation of fast shear wave and the length of arrow is proportional to magnitude of splitting. The bottom figure shows δt as a function of latitude.

with the expectation that more melt is expected towards the mature Afar Depression. Building on this study and later SKS splitting analyses in Ethiopia (e.g. Gashawbeza *et al.* 2004; Kendall *et al.* 2005, 2006), Bastow *et al.* (2010) combined analysis of surface and body waves to show that three mechanisms for anisotropy act beneath the Ethiopian rift: periodic thin layering of seismically fast and slow material in the uppermost *c.* 10 km; oriented melt pockets (with aspect ratio *c.* 0.02) at *c.* 20–75 km depth; and olivine LPO in the upper mantle beneath. The results are explained best by a model in which low-aspect-ratio melt inclusions (dykes and veins) are being intruded into an extending plate during late stage break-up (Bastow *et al.* 2010). In conjunction with the results on crustal structure (see 'Eastern Africa' section) these observations from Ethiopia again show that magma plays an important role in accommodating strain during the late stages of continental break-up. In northern Afar, where the strain field is characterized by the subaerial Red Sea and Gulf of Aden rifts, two anisotropic layers are identified in SKS shear-wave splitting analysis (Gao *et al.* 2010): the upper layer, interpreted as WNW-trending dyke intrusions; and the lower layer with a stronger NE-trending anisotropic fabric, interpreted as LPO due to horizontal flow in the mantle beneath the extending plate.

The extent to which the mantle beneath east Africa has a vertical flow component is unclear from the body-wave studies, because the method delivers only null measurements when anisotropic fabrics are perpendicular to the shear-wave particle motion. However, using data from both Rayleigh and Love waves, surface-wave studies can estimate the variation in radial anisotropy (the difference in velocity between vertically and horizontally propagating shear waves). Montagner *et al.* (2007) and Sicilia *et al.* (2008) find low values of radial anisotropy beneath Afar which, combined with the slow wave speeds, indicates an upwelling consistent with geodynamic models that also points towards a vertical and thus buoyant component of the flow field. These surface-wave studies also show a complex pattern of azimuthal anisotropy with significant variations of fast direction with depth, not completely consistent with the SKS results.

Southern Africa. Shear-wave splitting observations from the SASE experiment in southern Africa were some of the first to show that Archaean mantle deformation could be preserved as fossil mantle anisotropy (Silver *et al.* 2001): fast polarization directions systematically follow the trend of Archaean structures. The most anisotropic regions are Late Archaean in age (Zimbabwe Craton, Limpopo Belt, western Kaapvaal Craton), with δt reducing dramatically in off-craton regions to the

SW and Early Archaean regions to the SE (Fig. 8). Silver *et al.* (2001) also proposed that small or vertically incoherent seismic anisotropy was a likely explanation for the Early Archaean regions of southern Africa. In contrast, Freybourger *et al.* (2001) modelled the structure beneath the array using surface-wave data; azimuthal anisotropy compatible with the SKS results was not observed at periods sensitive to lithospheric mantle depths. Radial anisotropy, with SH faster than SV in the top 100 km, was however required to fit the data.

Below the thick lithosphere of southern Africa, one estimate of seismic anisotropy comes from the detailed analysis of converted phases (Vinnik *et al.* 2009); interpretation of these results indicated a NE fast direction at *c.* 300 km depth. Given the inferred depth to this anisotropy and correlation with plate motion, it has been related to deformation of the base of the lithosphere or an asthenospheric fabric. In the continental-scale study by Sebai *et al.* (2006) radial anisotropy is positive beneath southern Africa, although the anisotropy extends to greater depths than in the model of Freybourger *et al.* (2001), and the Love wave path coverage is limited. There is therefore no strong evidence for vertical upwelling acting as a support for the southern Africa topographic high.

Northern, central and western Africa. In the rest of Africa there have been no local-to-regional studies of seismic anisotropy. Given the evidence for slow velocities and possible mantle upwelling beneath the Cameroon Volcanic Line (see 'Northern, central and western Africa' section), detailed estimates of radial anisotropy could provide fundamental constraints on the extent of vertical flow. Similarly, the geodynamic modelling of Forte *et al.* (2010) indicates significant upwelling from a region termed the West African Superplume. Further measurements of anisotropy in this region would improve the understanding of the contribution to topography of the mantle flow fields.

Discussion and outlook

Seismic data can help constrain a number of factors that are fundamental to the cause and support of Africa's topography. Receiver function analysis, for example, can help constrain crustal thickness and density variations. These in turn are essential to appreciate what proportion of the observed topography is isostatically compensated. Mantle velocities, revealed using seismic tomography, are readily interpreted in terms of temperature variations and buoyancy. Coupled with measurements of seismic anisotropy, which place constraints on the direction of mantle flow, these observations help to identify regions where topography is

dynamically supported. With the inclusion of receiver function study of the mantle transition zone, seismological observations can also be used to link some regions of high topography and recent volcanism to upwellings that originate in the lower mantle. Given constraints on topography on the LAB, the geodynamicist can also constrain more subtle effects on topography from edge-driven mantle convection; this level of investigation is however only possible via a suite of seismological observations.

We now know from global-to-regional seismic tomographic inversions that the mantle beneath eastern and southern Africa is characterized by a broad low-velocity zone that extends from the core mantle boundary beneath southern Africa and impinges on the LAB somewhere in the region of Ethiopia. Geodynamic and seismic studies (e.g. Lithgow-Bertelloni & Silver 1999; Gurnis *et al.* 2000; Daradich *et al.* 2003; Simmons *et al.* 2007; Forte *et al.* 2010) each show that the mantle flow field is important in explaining the first-order super-swell topography. Detailed correlations of dynamic topography, however, require a calculation of the isostatically compensated topography. Nyblade & Robinson (1994) used average elevation on the continents and the expected bathymetry to estimate the residual topography for the African superswell, and this residual was matched in the studies of Lithgow-Bertelloni & Silver (1999) and Gurnis *et al.* (2000). The recent seismic tomography of Simmons *et al.* (2009) and geodynamic modelling of Forte *et al.* (2010) use estimates of dynamic topography as a constraint on their models. In these cases the isostatic topography is estimated from the Crust2.0 model (Bassin *et al.* 2000).

Figure 3 shows that when compared to the relatively smooth continent-scale crustal model of Pasyanos & Nyblade (2007) derived using surface-wave data, Crust2.0 provides very different *a priori* constraints on crustal structure. The model of Pasyanos & Nyblade (2007) for example shows generally thicker crust in the southern half of the African continent, as might be expected due to the high topography. This bimodality in crustal thickness is not, however, observed in Crust2.0 (Bassin *et al.* 2000). Fortunately, the ever-growing body of literature reporting on regional variations in crustal thickness in Africa means that future geodynamic models should be able to place tighter *a priori* constraints on the crust.

Despite these uncertainties at a continental scale, dense seismic networks have successfully improved our understanding of regional topographic variation. In Ethiopia, for example, where controlled-source (e.g. Keranen *et al.* 2004; Maguire *et al.* 2006) and passive-source seismic study (e.g. Dugda *et al.* 2005; Daly *et al.* 2008) provides detailed

constraints on the structure across the EAR, modelling of the gravity field has been successful in resolving fine-scale variations in crustal density (e.g. Cornwell *et al.* 2006; Mickus *et al.* 2007). A well-resolved crust has led to a better-understood mantle: the observed low-density buoyant upper mantle (e.g. Bastow *et al.* 2008) is required beneath the under-plated uplifted Ethiopian Plateau and the Main Ethiopian Rift (MER) in order to account for the long-wavelength features of the gravity field (Cornwell *et al.* 2006). Consistent with these observations, thermochronological analysis of incision rates on the Ethiopian Plateau point strongly towards a mantle contribution to the observed plateau uplift (e.g. Pik *et al.* 2008).

While significant progress has been made in eastern Africa in understanding topography (see also Nyblade 2011), several challenges remain. Many tomographic studies provide only relative measures of seismic velocity because they invert relative and not absolute arrival-time data (e.g. Bastow *et al.* 2005, 2008; Benoit *et al.* 2006*c*; Park & Nyblade 2006). Linkage of these low-velocity zones to the lower mantle is also unclear from receiver function analyses of 410 and 660 km discontinuities that do not, as yet, confidently identify broad regions where the transition zone is thinned due to elevated temperatures. Despite these and other remaining questions in east Africa, given the number of seismic experiments and interdisciplinary studies it is perhaps unsurprising that eastern Africa is now the best understood region of the continent.

Elsewhere, correlations between seismic results and topography are often unclear. In southern Africa, for example, local crustal thickness variations within the Kaapvaal Craton are not matched by changes in topography (Webb *et al.* 2004; Yang *et al.* 2008). Furthermore, the cause and extent of the observed upper mantle low-velocity zone remains ambiguous (e.g. Savage & Silver 2008; Hansen *et al.* 2009*b*), and the observations within the MTZ do not indicate a present-day link to the underlying superplume (Stankiewicz *et al.* 2002). Recent geodynamic models that incorporate chemical heterogeneity to the mantle density field also find no present-day dynamic uplift beneath much of southern Africa (Forte *et al.* 2010). There remains no single, unambiguous explanation for the broad region of high topography in southern Africa.

Many of the smaller-scale topographic features (Fig. 1) such as the volcanic swells of north Africa, the Atlas Mountains, the Cameroon Volcanic Line and the swells around the margin of southern Africa are underlain by low velocities in the uppermost mantle (e.g. King & Ritsema 2000; Montagner *et al.* 2007; Al-Hajri *et al.* 2009;

Reusch *et al.* 2010; Fig. 5). These topographic features are often located close to abrupt changes in lithospheric thickness (e.g. Priestley *et al.* 2008; Fishwick 2010; Fig. 6) and edge-driven convection may therefore influence topography in these regions (King & Ritsema 2000; Reusch *et al.* 2010). Alternatively, these rapid variations in lithospheric thickness could act as a guide to the larger-scale mantle flow, focusing upwellings at the margin of cratonic regions.

As the volume of seismic data from Africa continues to increase many of these issues will be addressed, adding fundamental new constraints to future generations of geodynamic models. To conclude, we highlight a number of key seismic observations and methodologies that will be particularly important in establishing improved links between seismological and topographic variations.

(1) Continent-wide high-resolution measurements of crustal thickness and density are required for accurate quantification of Africa's isostatically compensated topography. This goal will be achieved best via receiver function analysis at future dense deployments across the continent, although improved surface-wave studies will also help. Residual topography, in the absence of compressional tectonics, can then be attributed more confidently to mantle effects.

(2) In order to understand the effects of the mantle in dynamically supporting topography, improved tomographic images of mantle structure will be required. The development of techniques to estimate absolute velocities from regional body-wave studies to replace the present generation of relative arrival-time models will help constrain physical properties (density, viscosity, etc.) of the mantle more accurately.

(3) Ray tracing through these updated 3D tomographic models, rather than a 1D Earth model, will help remove the effects of upper mantle heterogeneity and thus sharpen migrated images of the transition zone revealed by receiver function analysis. The resulting maps of P660s-P410s will subsequently help identify uplifted and volcanically active regions where upper-mantle low velocities are sourced from the lower mantle.

(4) Understanding small-scale convection patterns in the asthenosphere can be appreciated only when variations in lithospheric thickness are constrained better from combined surface wave and receiver function study. These lateral variations in lithospheric structure then need to be incorporated in future generations of geodynamic models. The related lateral changes in temperature, density and, particularly, viscosity may have profound implications for the flow regime in the uppermost mantle.

(5) Estimates of seismic anisotropy become increasingly important to validate the geodynamical modelling. Improved resolution of Love wave velocities is needed to determine shorter-wavelength features of radial anisotropy. Shear-wave splitting measurements provide short-length-scale constraints on the direction of the flow field, and concurrent analyses of these data with estimates of azimuthal anisotropy from surface waves will help separate lithospheric and asthenospheric contributions to the observations. The latter will provide benchmark constraints for future geodynamic models that predict the flow field.

It is clear that while seismic studies can provide a number of important constraints, it is only through the integration of many areas of Earth sciences that a full understanding of Africa's varied topography will emerge.

Appendix

Table A1. *Compilation of Moho depth estimates from receiver functions and joint inversion of receiver functions and surface-wave dispersion data (see Fig. 4)*

Southern Africa				Southern Africa			
Station	Latitude	Longitude	Depth (km)	Station	Latitude	Longitude	Depth (km)
SA01	−34.29	19.25	26[b], 30.0[c]	SA53	−24.11	29.33	43[a]
SA02	−33.74	20.27	44[b], 38.5[c]	SA54	−23.72	30.67	35.5[a], 38.0[c]

(Continued)

Table A1. *Continued*

Southern Africa				Southern Africa			
Station	Latitude	Longitude	Depth (km)	Station	Latitude	Longitude	Depth (km)
SA03	−33.66	21.34	36–44[b], 48.7[c]	SA55	−22.98	28.3	43[a], 42.7[c]
SA04	−32.85	19.62	25.5[a], 36–44[b]	SA56	−23.01	29.07	43[a], 41.7[c]
SA05	−32.61	21.54	25.5[a], 40–45[b], 44.1[c]	SA57	−22.98	30.02	40.5[a], 40.3[c]
SA07	−31.98	20.23	41–46[b], 46.2[c]	SA58	−23.52	31.4	43.7[c]
SA08	−31.91	22.07	50[b], 49.3[c]	SA59	−24.84	24.46	40.5[a], 41.0[c]
SA09	−30.92	22.99	38[a], 46[b], 47.6[c]	SA60	−23.85	24.96	40.5[a], 41.1[c]
SA10	−30.97	23.91	33.0[a], 45.5[a], 42–46[b], 46.8[c]	SA61	−23.95	24.02	43[a], 43.2[c]
SA11	−29.97	20.95	40.5[a], 41.4[c]	SA62	−24.85	25.14	40.5[a], 41.3[c]
SA12	−29.85	22.25	43.9[c]	SA63	−23.66	26.08	43[a], 42.3[c]
SA13	−29.98	23.14	35.5[a], 35.9[c]	SA64	−22.97	26.2	40.5[a], 41.2[c]
SA14	−29.87	24.02	33[a], 34.2[c]	SA65	−22.82	27.22	40.5[a], 43.0[c]
SA15	−29.9	25.03	35.5[a], 36.4[c]	SA66	−21.9	26.37	38.0[a], 48.0[a], 46.9[c]
SA16	−28.95	22.2	40.5[a], 34.7[c]	SA67	−21.89	27.27	45.5[a]
SA17	−28.93	23.23	35.5[a], 38.0[c]	SA68	−21.95	28.19	45.5[a], 50.3[c]
SA18	−28.63	24.31	35.5[a], 36.5[c]	SA69	−22.31	29.27	52.6[c]
SA19	−28.91	24.83	35.5[a], 36.6[c]	SA70	−21.09	26.34	50.5[a], 51.6[c]
SA20	−29.02	26.2	35.5[a], 36.4[c]	SA71	−20.93	27.14	43[a], 43.6[c]
SA22	−27.97	22.01	35.5[a], 48.0[a]	SA72	−20.14	28.61	35.5[a], 37.7[c]
SA23	−27.93	23.41	40.5[a], 40.4[c]	SA73	−21.85	30.28	35.5[a], 45.5[a], 49.6[c]
SA24	−27.88	24.24	38[a], 38.4[c]	SA74	−21.92	30.93	40.5[a], 42.2[c]
SA25	−27.85	25.13	38[a], 37.8[c]	SA75	−20.86	29	37.5[a], 39.0[c]
SA26	−27.55	26.18	37.5[a], 39.1[c]	SA76	−20.64	29.85	35.5[a], 36.5[c]
SA27	−27.86	27.29	37.5[a], 39.1[c]	SA77	−20.76	30.92	38[a], 39.0[c]
SA28	−27.9	28.07	37.5[a], 37.4[c]	SA78	−19.47	30.77	35.5[a], 37.2[c]
SA29	−26.93	23.04	35.5[a], 35.8[c]	SA79	−20.02	30.52	37.5[a], 37.7[c]
SA30	−27.07	24.17	35.5[a], 36.6[c]	SA80	−19.96	31.32	35.5[a], 37.5[c]
SA31	−27	25.02	38[a], 38.5[c]	SA81	−30.93	21.27	33[a], 42–46[b], 46.6[c]
SA32	−26.87	26.28	37.5[a], 38.9[c]	SA82	−30.98	22.25	42–48[b], 49.1[c]
SA33	−26.9	27.18	37.5[a], 37.6[c]	POGA	−27.35	31.71	33.0[a], 40.5[a]
SA34	−26.8	28.1	35.5[a], 37.5[c]	HVD	−30.61	25.5	35.5[a]
SA35	−27.02	29.09	40.5[a], 39.6[c]	SEK	−28.32	27.63	37.5[a]
SA36	−26.88	30.13	38[a], 36.5[c]	MOPA	−23.52	31.4	35.5[a], 43.0[a]
SA37	−25.97	23.72	33[a], 34.6[c]	SWZ	−27.18	25.33	38[a]
SA38	−25.93	25.09	38[a], 39.2[c]	UPI	−28.36	21.25	40.5[a]
SA39	−25.9	26.15	40.5[a], 41.7[c]	CVNA	−31.48	19.76	28[a]
SA40	−25.9	27.15	43[a], 44.5[c]	GRM	−33.31	26.57	28.0[a], 35.5[a]
SA42	−25.67	29.22	38[a], 42.0[c]	BB02	−28.38	24.59	40.5[a]
SA43	−25.79	30.07	35.5[a], 43.0[a], 43.3[c]	BB08	−28.43	24.63	35.5[a]
SA44	−26.03	30.9	25.5[a], 40.5[a], 41.2[c]	BB14	−28.54	24.68	38[a]
SA45	−24.88	26.16	45.5[a], 43.8[c]	BB24	−28.62	24.63	35.5[a]
SA46	−24.84	27.11	40.5[a], 39.4[c]	BB31	−28.79	24.93	35.5[a]
SA47	−24.85	28.16	45.5[a], 48.9[c]	BOSA	−28.61	25.56	35.5[a], 35.8[c]
SA48	−24.9	29.22	45.5[a], 45.2[c]	LBTB	−25.02	25.6	43[a], 41.4[c]
SA49	−24.96	30.31	38[a], 53.5[c]	SUR	−32.38	20.81	35.5[a], 42–46[b], 49.2[c]
SA50	−23.87	27.17	38[a], 39.7[c]				
SA51	−23.86	28.16	43[a], 48.9[c]				
SA52	−23.8	28.9	38[a], 39.7[c]				

Western Africa				Eastern Africa			
Station	Latitude	Longitude	Depth (km)	Station	Latitude	Longitude	Depth (km)
CM01	2.39	9.83	28[d]	NYAN	0.21	30.45	32[e]
CM02	2.7	13.29	43[d]	RUBO	0.34	30.04	21[e]
CM03	3.52	15.03	43[d]	RUGA	−0.26	30.1	38[e]
CM04	2.98	11.96	45.5[d]	RWEB	0.32	30.49	32[e]
CM05	2.94	9.91	28[d]	SEML	0.91	30.36	34[e]

(*Continued*)

Table A1. *Continued*

Western Africa					Eastern Africa		
Station	Latitude	Longitude	Depth (km)	Station	Latitude	Longitude	Depth (km)
CM06	2.39	11.27	45.5[d]	SEMP	0.84	30.17	27[e]
CM07	3.87	11.46	43[d]	ANGA	−2.5	36.8	39[f]
CM09	4.23	9.33	25.5[d], 40.5[d]	KAKA	0.56	34.8	37[f]
CM10	4.22	10.62	38[d]	KITU	−1.37	38	40[f]
CM11	3.98	13.19	48[d]	KMBO	−1.13	37.25	41[f]
CM12	4.48	11.63	38[d]	KR42	0.04	35.73	38[f]
CM13	4.59	9.46	28[d]	NAI	−2.37	36.8	42[f]
CM15	5.03	9.93	33[d]	TALE	0.98	34.98	38[f]
CM16	5.48	10.57	35.5[d]	BASO	−4.32	35.14	41[g]
CM17	5.55	12.31	35.5[d]	MBWE	−4.96	34.35	37[g]
CM18	5.72	9.36	30.5[d]	MITU	−6.02	34.06	38[g]
CM19	5.98	11.23	35.5[d]	MTAN	−7.91	33.32	37[g]
CM20	6.23	10.05	33[d]	MTOR	−5.25	35.4	38[g]
CM21	6.47	12.62	35.5[d]	PUGE	−4.72	33.18	37[g]
CM22	6.48	13.27	35.5[d]	RUNG	−6.94	33.52	42[g]
CM23	6.37	10.79	40.5[d]	SING	−4.64	34.73	37[g]
CM24	6.52	14.29	35.5[d]	HALE	−5.3	38.62	39[g]
CM25	6.76	11.81	38[d]	KIBA	−5.32	36.57	36[g]
CM26	7.27	13.55	33[d]	KIBE	−5.38	37.48	37[g]
CM27	7.36	12.67	35.5[d]	KOMO	−3.84	36.72	36[g]
CM28	8.47	13.24	30.5[d]	KOND	−4.9	35.8	37[g]
CM29	9.35	13.39	25.5[d]	LONG	−2.73	36.7	37[g]
CM30	9.76	13.95	28[d]	TARA	−3.89	36.02	37[g]
CM31	10.33	15.26	30.5[d]	GOMA	−4.84	29.69	44[g]
CM32	10.62	14.37	33[d]	INZA	−5.12	30.4	42[g]
				PAND	−8.98	33.24	35[g]
				BURO	0.86	30.17	24[e]
				ITOJ	0.84	30.23	21[e]
				KABA	0.78	30.13	24[e]
				KABE	0.87	30.47	34[e]
				KABG	0.63	30.65	30[e]
				KAGO	0.68	30.46	32[e]
				KARA	0.09	29.9	28[e]
				KARU	0.79	30.22	21[e]
				KASE	−0.03	30.15	30[e]
				KASS	0.57	30.31	24[e]
				KILE	0.21	30.01	22[e]
				KISA	0.59	30.74	30[e]
				KMTW	0.74	30.38	30[e]
				MBAR	−0.6	30.74	30[e], 33[f]
				MIRA	0.66	30.57	29[e]
				MWEY	−0.19	29.9	28[e]
				NGIT	0.64	30.03	25[e]

Ethiopia					Ethiopia		
Station	Latitude	Longitude	Depth (km)	Station	Latitude	Longitude	Depth (km)
ADEE	7.79	39.91	37.6[h]	AAUS	9.04	38.77	37[f]
ADUE	8.54	38.9	33.9[h]	ARBA	6.07	37.56	30[f]
AMME	8.3	39.09	37.6[h]	BELA	6.93	38.47	38[f]
ANKE	9.59	39.73	37.6[h]	BIRH	9.67	39.53	41[f]
AREE	8.93	39.42	33.6[h]	DMRK	10.31	37.73	41[f]
ASEE	7.97	39.13	38.2[h]	GOBA	7.03	39.98	42[f]
AWAE	8.99	40.17	36.0[h]	GUDE	8.97	37.77	36.5[f]
BEDE	8.91	40.77	41.9[h]	HERO	7.03	39.28	42[f]

(Continued)

Table A1. *Continued*

Ethiopia				Ethiopia			
Station	Latitude	Longitude	Depth (km)	Station	Latitude	Longitude	Depth (km)
BORE	8.73	39.55	32.0[h]	HIRN	9.22	41.11	41[f]
BUTE	8.12	38.38	32.0[h]	HOSA	7.56	37.86	37[f]
CHAE	9.31	38.76	40.7[h]	JIMA	7.68	36.83	36[f]
DIKE	8.06	39.56	42.6[h]	KARA	10.42	39.94	44[f]
DZEE	8.78	39	38.4[h]	NAZA	8.57	39.29	27[f]
FURI	8.9	36.69	37.4[f], 37.4[h]	NEKE	9.09	36.52	34[f]
GTFE	8.99	39.84	31.4[h]	SELA	7.97	39.13	27[f]
INEE	9.9	39.14	40.7[h]	WANE	10.17	40.65	30[f]
HIRE	9.22	41.11	39.4[h]	WASH	8.99	40.17	35[f]
KARE	10.42	39.94	43.8[h]	WELK	8.3	37.78	33[f]
KOTE	9.39	39.4	45.7[h]	BAHI	11.57	37.39	44[f]
LEME	8.61	38.61	33.3[h]	CHEF	6.16	38.21	37[f]
MECE	8.59	40.32	37.6[h]	DELE	8.44	36.33	36[f]
MELE	9.31	40.2	35.0[h]	DIYA	11.83	39.6	37[f]
MIEE	9.24	40.76	35.0[h]	TEND	11.79	41	25[f]
NURE	8.7	39.8	32.6[h]	TERC	7.15	37.18	34[f]
SENE	9.15	39.02	41.9[h]	1179	8.85	39.24	35.8[i]
SHEE	10	39.9	35.9[h]	1246	8.5	39.57	38.2[i]
E31	8.78	39.86	35.4[h]	1266	8.36	39.67	35.5[i]
E32	8.85	40.01	35.2[h]	1281	8.25	39.7	36.4[i]
E33	8.93	39.93	35.5[h]	1296	8.13	39.72	38.6[i]
E34	7.21	38.6	38.9[h]	1306	8.05	39.69	40.1[i]
E35	9.13	40.17	34.3[h]	1324	7.93	39.75	41.1[i]
E36	9.11	40.01	35.0[h]	1333	7.87	39.81	41.0[i]
E40	9.36	40.22	35.0[h]	1337	7.85	39.84	40.4[i]
E50	8.27	39.5	36.9[h]	1351	7.78	39.94	38.9[i]
E51	8.15	39.35	38.6[h]	1373	7.71	40.14	37.5[i]
E52	8.14	39.24	38.6[h]	1400	7.38	40.17	38.8[i]
E55	8.3	38.95	38.3[h]	E59	8.71	39.35	32.3[i]
E57	8.59	39.13	37.3[h]				
E64	8.57	39.29	33.6[h]				
E67	8.38	39.68	37.0[h]				
E70	8.88	39.15	35.7[h]				
E71	8.69	38.9	33.9[h]				
E72	8.49	39.83	38.4[h]				
E76	7.73	38.65	40.2[h]				
E79	7.64	38.72	39.2[h]				

[a]Kgaswane *et al.* (2009); [b]Harvey *et al.* (2001); [c]Nair *et al.* (2006); [d]Tokam *et al.* (2010); [e]Wölbern *et al.* (2010); [f]Dugda *et al.* (2005); [g]Last *et al.* (1997); [h]Stuart *et al.* (2006); [i]Cornwell *et al.* 2010.

References

ACHAUER, U. & MASSON, F. 2002. Seismic tomography of continental rifts revisited: from relative to absolute heterogeneities. *Tectonophysics*, **358**, 17–37.

AL-HAJRI, Y., WHITE, N. & FISHWICK, S. 2009. Scales of transient convective support beneath Africa. *Geology*, **37**, 883–886.

ARMITAGE, J. J. & ALLEN, P. A. 2010. Cratonic basins and the long-term subsidence history of continental interiors. *Journal of the Geological Society, London*, **167**, 61–70.

ASHWAL, L. D. & BURKE, K. 1989. African lithospheric structure, volcanism, and topography. *Earth and Planetary Science Letters*, **96**, 8–14.

AYADI, A., DORBATH, C., LESQUER, A. & BEZZEGHOUD, M. 2000. Crustal and upper mantle velocity structure of the Hoggar swell (Central Sahara), Algeria. *Physics of the Earth and Planetary Interiors*, **118**, 111–123.

AYALEW, D., BARBEY, P., MARTY, B., REISBERG, L., YIRGU, G. & PIK, R. 2002. Source, genesis, and timing of giant ignimbrite deposits associated with Ethiopian continental flood basalts. *Geochimica et Cosmochimica Acta*, **66**, 1429–1448.

AYELE, A., STUART, G. & KENDALL, J.-M. 2004. Insights into rifting from shear wave splitting and receiver functions; an example from Ethiopia. *Geophysical Journal International*, **157**, 354–362.

BASSIN, C., LASKE, G. & MASTERS, G. 2000. The current limits of resolution for surface wave tomography in North America. *Eos, Transactions, American Geophysical Union*, **81**, F897.

BASTOW, I. D., STUART, G. W., KENDALL, J. M. & EBINGER, C. J. 2005. Upper-mantle seismic structure in a region of incipient continental breakup: northern Ethiopian rift. *Geophysical Journal International*, **162**, 479–493.

BASTOW, I. D., NYBLADE, A. A., STUART, G. W., ROONEY, T. O. & BENOIT, M. H. 2008. Upper mantle seismic structure beneath the Ethiopian hotspot: rifting at the edge of the African low velocity anomaly. *Geochemistry, Geophysics, Geosystems*, **9**, Q12022, doi: 10.1029/2008GC002107.

BASTOW, I. D., PILIDOU, S., KENDALL, J. M. & STUART, G. W. 2010. Melt-induced seismic anisotropy and magma assisted rifting in Ethiopia: evidence from surface waves. *Geochemistry, Geophysics, Geosystems*, **11**, Q0AB05, doi: 10.1029/2010GC003036.

BASTOW, I. D., KEIR, D. & DALY, E. 2011. The Ethiopia Afar Geoscientific Lithospheric Experiment (EAGLE): probing the transition from continental rifting to incipient sea floor spreading. *In*: BECCALUVA, L., BIANCHINI, G. & WILSON, M. (eds) *Volcanism and Evolution of the African Lithosphere*. Geological Society of America, Special Papers, **478**, 51–76.

BEGG, G. C., GRIFFIN, W. L. ET AL. 2009. The lithospheric architecture of Africa: seismic tomography, mantle petrology and tectonic evolution. *Geosphere*, **5**, 23–50.

BEHN, M. D., CONRAD, C. P. & SILVER, P. G. 2004. Detection of upper mantle flow associated with the African Superplume. *Earth and Planetary Science Letters*, **224**, 259–274.

BENOIT, M., NYBLADE, A., OWENS, T. & STUART, G. 2006*a*. Mantle transition zone structure and upper mantle S velocity variations beneath Ethiopia: evidence for a broad, deep-seated thermal anomaly. *Geochemistry, Geophysics, Geosystems*, **7**, Q10113, doi: 10.1029/2006GC001398.

BENOIT, M., NYBLADE, A. & PASYANOS, M. 2006*b*. Crustal thinning between the Ethiopian and East African Plateaus from modeling Rayleigh wave dispersion. *Geophysical Research Letters*, **33**, L13301, doi: 10.1029/2006GL025687.

BENOIT, M., NYBLADE, A. & VANDECAR, J. 2006*c*. Upper mantle P wavespeed variations beneath Ethiopia and the origin of the Afar hotspot. *Geology*, **34**, 329–332.

BINA, C. R. & HELFFRICH, G. 1994. Phase transition Clapeyron slopes and transition zone seismic discontinuity topography. *Journal of Geophysical Research*, **99**, 15853–15860.

BLACKMAN, D. & KENDALL, J. M. 1997. Sensitivity of teleseismic body waves to mineral texture and melt in the mantle beneath a mid-ocean ridge. *Philosophical Transactions of the Royal Society, London*, **355**, 217–231.

BRAUN, J. 2010. The many surface expressions of mantle dynamics. *Nature Geoscience*, **3**, 825–833.

BROWN, R. W., SUMMERFIELD, M. A. & GLEADOW, A. J. W. 2002. Denudational history along a transect across the Drakensberg Escarpment of southern Africa derived from apatite fission-track thermochronology. *Journal of Geophysical Research*, **107**, doi: 10.1029/2001JB000745.

BUITER, S. J. H., PFIFFNER, O. A. & BEAUMONT, C. 2009. Inversion of extensional sedimentary basins: a numerical evaluation of the localisation of shortening. *Earth and Planetary Science Letters*, **288**, 492–504.

BURKE, K. 1996. The African plate. *South African Journal of Geology*, **99**, 341–409.

CARLSON, R. W., GROVE, T. L., DE WIT, M. J. & GURNEY, J. J. 1996. Anatomy of an Archean craton: a program for interdisciplinary studies of the Kaapvaal Craton, southern Africa. *Eos, Transactions, American Geophysical Union*, **77**, 273–277.

CHEVROT, S. & ZHAO, L. 2007. Multiscale seismic tomography finite-frequency Rayleigh wave tomography of the Kaapvaal craton. *Geophysical Journal International*, **169**, 201–215.

CORNWELL, D. G., MACKENZIE, G. D., ENGLAND, R. W., MAGUIRE, P. K. H., ASFAW, L. M. & OLUMA, B. 2006. Northern Main Ethiopian Rift crustal structure from new high precision gravity data. *In*: YIRGU, G., EBINGER, C. J. & MAGUIRE, P. K. H. (eds) *The Afar Volcanic Province within the East African Rift System*. Geological Society, London, Special Publications, **256**, 307–321.

CORNWELL, D. G., MAGUIRE, P. K. H., ENGLAND, R. W. & STUART, G. W. 2010. Imaging detailed crustal structure and magmatic intrusion across the Ethiopian rift using a dense linear broadband array. *Geochemistry, Geophysics, Geosystems*, **11**, Q0AB03, doi: 10.1029/2009GC002637.

COULIE, E., QUIDELLEUR, P. Y., GILLOT, P. Y., COURTILLOT, V., LEFÈVRE, J. C. & CHIESA, S. 2003. Comparative K–Ar and Ar–Ar dating of Ethiopian and Yemenite Oligocene volcanism: implications for timing and duration of the Ethiopian traps. *Earth and Planetary Science Letters*, **206**, 477–492.

CROSBY, A., FISHWICK, S. & WHITE, N. 2010. Structure and evolution of the intracratonic Congo Basin. *Geochemistry, Geophysics, Geosystems*, **11**, Q06010, doi: 10.1029/2009GC003014.

DALY, E., KEIR, D., EBINGER, C. J., STUART, G. W., BASTOW, I. D. & AYELE, A. 2008. Crustal tomographic imaging of a transitional continental rift: the Ethiopian rift. *Geophysical Journal International*, **172**, 1033–1048.

DALY, M. C., LAWRENCE, S. R., DIEMU-TSHIBAND, K. & MATOUANA, B. 1992. Tectonic evolution of the Cuvette Centrale, Zaire. *Journal of the Geological Society, London*, **149**, 539–546.

DARADICH, A., MITROVICA, J., PYSKLYWEC, R., WILLETT, S. & FORTE, A. 2003. Mantle flow, dynamic topography, and rift-flank uplift of Arabia. *Geology*, **31**, 901–904.

DE WIT, M. 2007. The Kalahari Epeirogeny and climate change: dfferentiating cause and effect from core to space. *South African Journal of Geology*, **110**, 367–392.

DEBAYLE, E., LÉVÊQUE, J.-J. & CARA, M. 2001. Seismic evidence for a deeply rooted low-velocity anomaly in the upper mantle beneath the northeastern Afro/Arabian continent. *Earth and Planetary Science Letters*, **193**, 423–436.

DEBAYLE, E., KENNETT, B. L. N. & PRIESTLEY, K. 2005. Global azimuthal seismic anisotropy: the unique plate-motion of Australia. *Nature*, **433**, 509–512.

DORBATH, C., DORBATH, L., FAIRHEAD, J. D. & STUART, G. W. 1986. A teleseismic delay time study across the

Central African Shear Zone in the Adamawa region of Cameroon, West Africa. *Geophysical Journal of the Royal Astronomical Society*, **86**, 751–766.

DOUCOURÉ, C. M. & DE WIT, M. J. 2003. Old inherited origin for the present near bimodal topography of Africa. *Journal of African Earth Sciences*, **36**, 371–388.

DOWNEY, N. J. & GURNIS, M. 2009. Instantaneous dynamics of the cratonic Congo basin. *Journal of Geophysical Research*, **114**, B06401, doi: 10.1029/2008JB006066.

DUGDA, M. T., NYBLADE, A. A., JULIÀ, J., LANGSTON, C. A., AMMON, C. A. & SIMIYU, S. 2005. Crustal structure in Ethiopia and Kenya from receiver function analysis: implications for rift development in eastern Africa. *Journal of Geophysical Research*, **110**, B01303, doi: 10.1029/2004JB003065.

DUGDA, M. T., NYBLADE, A. A. & JULIÀ, J. 2009. S-wave velocity structure of the crust and upper mantle beneath Kenya in comparison to Tanzania and Ethiopia: implications for the formation of the East African and Ethiopian plateaus. *South African Journal of Geology*, **112**, 241–250.

EBINGER, C. J. & SLEEP, N. H. 1998. Cenozoic magmatism throughout east Africa resulting from impact of a single plume. *Nature*, **395**, 788–791.

EBINGER, C., BECHTEL, T., FORSYTH, D. & BOWIN, C. 1989. Effective elastic plate thickness beneath the East African and Afar plateaus and dynamic compensation of the uplifts. *Journal of Geophysical Research*, **94**, 2883–2901.

FAUL, U. H. & JACKSON, I. 2005. Seismic signatures of temperature variations in the upper mantle. *Earth and Planetary Science Letters*, **234**, 119–134.

FISHWICK, S. 2010. Surface wave tomography: imaging of the lithosphere asthenosphere boundary beneath central and southern Africa. *Lithos*, **120**, 63–73.

FORTE, A., QUÉRÉ, S., MOUCHA, R., SIMMONS, N. A., GRAND, S. P., MITROVICA, J. X. & ROWLEY, D. B. 2010. Joint seismic-geodynamic-mineral physical modelling of African geodynamics: a reconciliation of deep-mantle convection with surface geophysical constraints. *Earth and Planetary Science Letters*, **295**, 329–341.

FOUCH, M. J., JAMES, D. E., VANDECAR, J. C., VAN DER LEE, S. & KAAPVAAL SEISMIC GROUP. 2004. Mantle seismic structure beneath the Kaapvaal and Zimbabwe Cratons. *South African Journal of Geology*, **107**, 33–44.

FREYBOURGER, M., GAHERTY, J. B., JORDAN, T. H. & THE KAAPVAAL SEISMIC GROUP. 2001. Structure of the Kaapvaal craton from surface waves. *Geophysical Research Letters*, **28**, 2489–2492.

FRIZON DE LAMOTTE, D., SAINT BEZAR, B., BRACÈNE, R. & MERCIER, E. 2000. The two main steps of the Atlas building and geodynamics of the western Mediterranean. *Tectonics*, **19**, 740–761.

FULLEA, J., FERNÁNDEZ, M., ZEYEN, H. & VERGÈS, J. 2007. A rapid method to map the crustal and lithospheric thickness using elevation, geoid anomaly and thermal analysis. Application to the Gibraltar Arc System, Atlas Mountains and adjacent zones. *Tectonophysics*, **430**, 97–117.

FURMAN, T., BRYCE, J., HANAN, B., YIRGU, G. & AYALEW, D. 2006. Heads and tails: 30 Million years

of the Afar plume. *In*: YIRGU, G., EBINGER, C. J. & MAGUIRE, P. K. H. (eds) *The Afar Volcanic Province within the East African Rift System*. Geological Society, London, Special Publications, **259**, 95–119.

GANI, N., GANI, M. & ABDELSALAM, M. 2007. Blue Nile incision on the Ethiopian Plateau: pulsed plateau growth, Pliocene uplift, and hominin evolution. *GSA Today*, **17**, 4–11.

GAO, S., DAVIS, P. *ET AL*. 1997. SKS splitting beneath the continental rift zones. *Journal of Geophysical Research*, **102**, 22781–22797.

GAO, S. S., LIU, K. H. & ABDELSALEM, M. G. 2010. Seismic anisotropy beneath the Afar Depression and adjacent areas: implications for mantle flow. *Journal of Geophysical Research*, **115**, B12330, doi: 10.1029/2009JB007141.

GASHAWBEZA, E., KLEMPERER, S., NYBLADE, A., WALKER, K. & KERANEN, K. 2004. Shear wave splitting in Ethiopia: Precambrian mantle anisotropy locally modified by Neogene rifting. *Geophysical Research Letters*, **31**, L18602, doi: 10.1029/2004GL020471.

GEORGE, R., ROGERS, N. & KELLEY, S. 1998. Earliest magmatism in Ethiopia: evidence for two mantle plumes in one continental flood basalt province. *Geology*, **26**, 923–926.

GIRESSE, P. 2005. Mesozoic–Cenozoic history of the Congo Basin. *Journal of African Earth Sciences*, **43**, 301–315.

GOES, S., CAMMARANO, F. & HANSEN, U. 2000. Shallow mantle temperatures under Europe from P and S wave tomography. *Journal of Geophysical Research*, **105**, 11153–11169.

GRAND, S. P. 2002. Mantle shear-wave tomography and the fate of subducted slabs. *Philosophical Transactions of the Royal Society*, **360**, 2475–2491.

GURNIS, M., MITROVICA, J. X., RITSEMA, J. & VAN HEIJST, H. J. 2000. Constraining mantle density structure using geological evidence of surface uplift rates: the case of the African superplume. *Geochemistry, Geophysics, Geosystems*, **1**, 1020, doi: 10.1029/1999GC000035.

HADIOUCHE, O. & JOBERT, N. 1988. Geographical distribution of surface-wave velocities and 3D upper mantle structure in Africa. *Geophysical Journal International*, **95**, 87–109.

HANKA, W., YUAN, X., KIND, R., WACKERLE, R., WYLEGALLA, K., BOCK, G. & TRUMBULL, R. 2000. First insights to upper mantle structure under the Damara Belt Namibia, from receiver function study. *Eos, Transactions, American Geophysical Union Supplement*, Fall Meeting Abstracts, F831.

HANSEN, S. E., NYBLADE, A. A. & JULIÀ, J. 2009a. Estimates of crustal and lithospheric thickness in sub-saharan Africa from S-wave receiver functions. *South African Journal of Geology*, **112**, 229–240.

HANSEN, S. E., NYBLADE, A. A., JULIÀ, J., DIRKS, P. H. G. M. & DURRHEIM, R. J. 2009b. Upper-mantle low-velocity zone structure beneath the Kaapvaal craton from S-wave receiver functions. *Geophysical Journal International*, **178**, 1021–1027.

HARTLEY, R. & ALLEN, P. A. 1994. Interior cratonic basins of Africa: relation to continental breakup and role of mantle convection. *Basin Research*, **6**, 95–113.

HARVEY, J. D., DE WIT, M. J., STANKIEWICZ, J. & DOUCOURÉ, C. M. 2001. Structural variations of the crust

in the Southwestern Cape, deduced from seismic receiver functions. *South African Journal of Geology*, **104**, 231–242.

HEINE, C., MÜLLER, R. D., STEINBERGER, B. & TORSVIK, T. H. 2008. Subsidence in intracontinental basins due to dynamic topography. *Physics of the Earth and Planetary*, **171**, 252–264.

HOFMANN, C., COURTILLOT, V., FERAUD, G., ROCHETTE, P., YIRGU, G., KETEFO, E. & PIK, R. 1997. Timing of the Ethiopian flood basalt event and implications for plume birth and global change. *Nature*, **389**, 838–841.

HOLMES, A. 1944. *Principles of Physical Geology*. Thomas Nelson and Sons Limited, Edinburgh.

HOLT, P., ALLEN, M. B., VAN HUSEN, J. & BJØRNSETH, H. M. 2010. Lithospheric cooling and thickening as a basin forming mechanism. *Tectonophysics*, **495**, 184–194.

JAMES, D. E., FOUCH, M. J., VANDECAR, J. C., VAN DER LEE, S. & KAAPVAAL SEISMIC GROUP. 2001. Tectospheric structure beneath southern Africa. *Geophysical Research Letters*, **28**, 2485–2488.

JORDAN, T. H. 1975. The continental tectosphere. *Reviews of Geophysics and Space Physics*, **13**, 1–12.

JULIÀ, J., AMMON, C. & NYBLADE, A. 2005. Evidence for mafic lower crust in Tanzania, East Africa, from joint inversion of receiver functions and Rayleigh wave dispersion velocities. *Geophysical Journal International*, **162**, 555–569.

KAMINSKI, E. & JAUPART, C. 2000. Lithosphere structure beneath the Phanerozoic intracratonic basins of North America. *Earth and Planetary Science Letters*, **178**, 139–149.

KAMINSKI, E. & RIBE, N. M. 2002. Timesclaes for the evolution of seismic anisoptropy in mantle flow. *Geochemistry, Geophysics, Geosystems*, **3**, 1051, doi: 10.1029/2001GC000222.

KEIR, D., BASTOW, I. D., WHALER, K. A., DALY, E., CORNWELL, D. G. & HAUTOT, S. 2009. Lower crustal earthquakes near the Ethiopian rift induced by magmatic processes. *Geochemistry, Geophysics, Geosystems*, **10**, Q0AB02, doi: 10.1029/2009GC002382.

KENDALL, J., STUART, G. W., EBINGER, C. J., BASTOW, I. D. & KEIR, D. 2005. Magma assisted rifting in Ethiopia. *Nature*, **433**, 146–148.

KENDALL, J., PILIDOU, S., KEIR, D., BASTOW, I. D., STUART, G. W. & AYELE, A. 2006. Mantle upwellings, melt migration and the rifting of Africa: insights from seismic anisotropy. *In*: YIRGU, G., EBINGER, C. J. & MAGUIRE, P. K. H. (eds) *The Afar Volcanic Province within the East African Rift System*. Geological Society, London, Special Publications, **259**, 55–72.

KENNETT, B. L. N., ENGDAHL, E. R. & BULAND, R. 1995. Constraints on seismic velocities in the Earth from travel times. *Geophysical Journal International*, **122**, 108–124.

KERANEN, K., KLEMPERER, S., GLOAGUEN, R. & EAGLE WORKING GROUP. 2004. Three dimensional seismic imaging of a protoridge axis in the main Ethiopian rift. *Geology*, **32**, 949–952.

KGASWANE, E. M., NYBLADE, A. A., JULIÀ, J., DIRKS, P. H. G. M., DURRHEIM, R. J. & PASYANOS, M. E. 2009. Shear wave velocity structure of the lower crust in southern Africa: evidence for compositional heterogeneity within Archaean and Proterozoic terrains. *Journal of Geophysical Research*, **114**, B12304, doi: 10.1029/2008JB006217.

KIEFFER, B., ARNDT, N. *ET AL.* 2004. Flood and shield basalts from Ethiopia: magmas from the African superswell. *Journal of Petrology*, **45**, 793–834.

KING, S. D. & ANDERSON, D. L. 1998. Edge-driven convection. *Earth and Planetary Science Letters*, **160**, 289–296.

KING, S. D. & RITSEMA, J. 2000. African hot spot volcanism: small-scale convection in the upper mantle beneath cratons. *Science*, **290**, 1137–1140.

KRISP WORKING GROUP. 1987. Structure of the Kenya rift from seismic refraction. *Nature*, **325**, 239–242.

LARSON, E. W. F. & EKSTRÖM, G. 2001. Global models of surface wave group velocity. *Pure and Applied Geophysics*, **158**, 1377–1399.

LAST, R. J., NYBLADE, A. A., LANGSTON, C. A. & OWENS, T. J. 1997. Crustal structure of the East African Plateau from receiver functions and Rayleigh wave phase velocities. *Journal of Geophysical Research*, **102**, 24469–24483.

LEBEDEV, S. & VAN DER HILST, R. D. 2008. Global upper-mantle tomography with the automated multimode inversion of surface and S-wave forms. *Geophysical Journal International*, **173**, 505–518.

LESQUER, A., TAKHERIST, D., DAUTRIA, J. M. & HADIOUCHE, O. 1990. Geophysical and petrological evidence for the presence of an 'anomalous' upper mantle beneath the Sahara basins (Algeria). *Earth and Planetary Science Letters*, **96**, 407–418.

LI, A. & BURKE, K. 2006. Upper mantle structure of southern Africa from Rayleigh wave tomography. *Journal of Geophysical Research*, **111**, B10303, doi: 10.1029/2006JB004321.

LI, C., VAN DER HILST, R. D., ENGDAHL, R. & BURDICK, S. 2008. A new global model for P wave speed variations in Earth's mantle. *Geochemistry, Geophysics, Geosystems*, **9**, Q05018, doi: 10.1029/2007GC001806.

LITHGOW-BERTELLONI, C. & SILVER, P. 1999. Dynamic topography, plate driving forces and the African superswell. *Nature*, **395**, 269–272.

LIU, K. H. & GAO, S. S. 2010. Spatial variations of crustal characteristics beneath the Hoggar swell, Algeria, revealed by systematic analyses of receiver functions from a single seismic station. *Geochemistry, Geophysics, Geosystems*, **11**, Q08011, doi: 10.1029/2010GC003091.

MACKENZIE, G. D., THYBO, H. & MAGUIRE, P. K. H. 2005. Crustal velocity structure across the Main Ethiopian Rift: Results from two-dimensional wide-angle seismic modelling. *Geophysical Journal International*, **162**, 994–1006.

MAGUIRE, P. K. H., EBINGER, C. J. *ET AL.* 2003. Geophysics project in Ethiopia studies continental breakup. *Eos, Transactions, American Geophysical Union*, **84**, 342–343.

MAGUIRE, P. K. H., KELLER, G. R. *ET AL.* 2006. Crustal structure of the northern Main Ethiopian Rift from the EAGLE controlled-source survey; a snapshot of incipient lithospheric break-up. *In*: YIRGU, G., EBINGER, C. J. & MAGUIRE, P. K. H. (eds) *The Afar Volcanic Province within the East African Rift System*. Geological Society, London, Special Publications, **259**, 269–292.

McKenzie, D. P. 1978. Some remarks on the development of sedimentary basins. *Earth and Planetary Science Letters*, **40**, 23–32.

Mechie, J., Keller, G. R., Prodehl, C., Khan, M. A. & Gaciri, S. J. 1997. A model for the structure, composition and evolution of the Kenya rift. *Tectonophysics*, **278**, 95–119.

Mickus, K., Tadesse, K., Keller, G. & Oluma, B. 2007. Gravity analysis of the main Ethiopian rift. *Journal of African Earth Sciences*, **48**, 59–69.

Montagner, J.-P., Marty, B. *et al.* 2007. Mantle upwellings and convective instabilities revealed by seismic tomography and helium isotope geochemistry beneath eastern Africa. *Geophysics Research Letters*, **34**, L21303, doi: 10.1029/2007GL031098.

Montelli, R., Nolet, G., Dahlen, F. & Masters, G. 2006. A catalogue of deep mantle plumes: new results from finite-frequency tomography. *Geochemistry, Geophysics, Geosystems*, **7**, Q110007, doi: 10.1029/2006GC001248.

Moorkamp, M., Jones, A. G. & Fishwick, S. 2010. Joint inversion of receiver functions, surface wave dispersion and magnetotelluric data. *Journal of Geophysical Research*, **115**, B04318, doi: 10.1029/2009JB006369.

Morley, C., Wescott, W., Stone, D., Harper, R., Wigger, S. & Karanja, F. 1992. Tectonic evolution of the northern Kenyan Rift. *Journal of the Geological Society*, **149**, 333.

Nair, S. K., Gao, S. S., Liu, K. H. & Silver, P. G. 2006. Southern African crustal evolution and composition: constraints from receiver function studies. *Journal of Geophysical Research*, **111**, B02304, doi: 10.1029/2005JB003802.

Nataf, H.-C. & Ricard, Y. 1996. 3SMAC: an a priori tomographic model of the upper mantle based on geophysical modeling. *Physics of the Earth and Planetary Interiors*, **95**, 101–122.

Nguuri, T. K., Gore, J. *et al.* 2001. Crustal structure beneath southern Africa and its implications for the formation and evolution of the Kaapvaal and Zimbabwe cratons. *Geophysics Research Letters*, **28**, 2501–2504.

Niu, F. & James, D. E. 2002. Fine structure of the lowermost crust beneath the Kaapvaal Craton and its implications for crustal formation and evolution. *Earth and Planetary Science Letters*, **200**, 121–130.

Nyblade, A. A. 2011. The upper mantle low velocity anomaly beneath Ethiopia, Kenya and Tanzania: Constraints on the origin of the African Superswell in eastern Africa and plate v. plume models of mantle dynamics. *In*: Beccaluva, L., Bianchini, G. & Wilson, M. (eds) *Volcanism and Evolution of the African Lithosphere*. Geological Society of America, Special Papers, **478**, 37–50.

Nyblade, A. & Robinson, S. 1994. The African superswell. *Geophysics Research Letters*, **21**, 765–768.

Nyblade, A. & Langston, C. A. 2002. Broadband seismic experiments probe the East African Rift. *Eos, Transactions, American Geophysical Union*, **83**, 405–408.

Nyblade, A. A. & Sleep, N. H. 2003. Long lasting epeirogenic uplift from mantle plumes and the origin of the Southern African Plateau. *Geochemistry, Geophysics, Geosystems*, **4**, 1105, doi: 10.1029/2003GC000573.

Nyblade, A., Birt, C., Langston, C. A., Owens, T. J. & Last, R. J. 1996. Seismic experiment reveals rifting of craton in Tanzania. *Eos, Transactions, American Geophysical Union*, **77**, 520–521.

Nyblade, A. A., Dirks, P., Durrheim, R., Webb, S., Jones, M., Cooper, G. & Graham, G. 2008. Africaarray: developing a geosciences workforce for africa's natural resource sector. *Leading Edge*, **27**, 1358–1361.

Park, Y. & Nyblade, A. 2006. P-wave tomography reveals a westward dipping low velocity zone beneath the Kenya Rift. *Geophysics Research Letters*, **33**, L07311, doi: 10.1029/2005GL025605.

Pasyanos, M. 2010. Lithospheric thickness modelled from long-period surface wave dispersion. *Tectonophysics*, **481**, 38–50.

Pasyanos, M. & Nyblade, A. A. 2007. A top to bottom lithospheric study of Africa and Arabia. *Tectonophysics*, **444**, 27–44.

Pedersen, H. A., Fishwick, S. & Snyder, D. B. 2009. A comparison of cratonic roots through consistent analysis of seismic surface waves. *Lithos*, **109**, 81–95.

Pérez-Gussinyé, M., Metois, M., Fernàndez, M., Vergés, J., Fullea, J. & Lowry, A. R. 2009. Effective elastic thickness of Africa and its relationship to other proxies for lithospheric structure and surface tectonics. *Earth and Planetary Science Letters*, **287**, 152–167.

Pik, R., Marty, B., Carignan, J. & Lavé, J. 2003. Stability of the Upper Nile drainage network (Ethiopia) deduced from (U–Th)/He thermochronometry: implications for uplift and erosion of the Afar plume dome. *Earth and Planetary Science Letters*, **215**, 73–88.

Pik, R., Marty, B. & Hilton, D. R. 2006. How many mantle plumes in Africa? The geochemical point of view. *Chemical Geolology*, **226**, 100–114.

Pik, R., Marty, B., Carignan, J., Yirgu, G. & Ayalew, T. 2008. Timing of East African Rift development in southern Ethiopia: implication for mantle plume activity and evolution of topography. *Geology*, **36**, 167–170.

Plomerová, J., Babuška, V., Dorbath, C., Dorbath, L. & Lillie, R. J. 1993. Deep lithospheric structure across the Central African Shear Zone in Cameroon. *Geophysical Journal International*, **115**, 381–390.

Poupinet, G. 1979. On the relation between P-wave travel time residuals and the age of the continental plates. *Earth and Planetary Science Letters*, **43**, 149–161.

Priestley, K. 1999. Velocity structure of the continental upper mantle: evidence from southern Africa. *Lithos*, **48**, 45–56.

Priestley, K. & McKenzie, D. 2006. The thermal structure of the lithosphere from shear wave velocities. *Earth and Planetary Science Letters*, **244**, 285–301.

Priestley, K. & Tillmann, F. 2009. Relationship between the upper mantle high velocity seismic lid and the continental lithosphere. *Lithos*, **109**, 112–124.

PRIESTLEY, K., McKENZIE, D., DEBAYLE, E. & PILIDOU, S. 2008. The African upper mantle and its relationship to tectonics and surface geology. *Geophysical Journal International*, **175**, 1108–1126.

PRODEHL, C. & MECHIE, J. 1991. Crustal thinning in relationship to the evolution of the Afro-Arabian rift system: a review of seismic refraction data. *Tectonophysics*, **198**, 311–327.

REUSCH, A. M., NYBLADE, A. A., WIENS, D. A., SHORE, P. J., ATEBA, B., TABOD, C. T. & NNANGE, J. M. 2010. Upper mantle structure beneath Cameroon from body wave tomography and the origin of the Cameroon Volcanic Line. *Geochemistry, Geophysics, Geosystems*, **11**, Q10W07, doi: 10.1029/2010GC003200.

RITSEMA, J. & VAN HEIJST, H. 2000. New seismic model of the upper mantle beneath Africa. *Geology*, **28**, 63–66.

RITSEMA, J. & ALLEN, R. M. 2003. The elusive mantle plume. *Earth and Planetary Science Letters*, **207**, 1–12.

RITSEMA, J., NYBLADE, A. A., OWENS, T. J., LANGSTON, C. A. & VANDECAR, J. C. 1998. Upper mantle seismic velocity structure beneath Tanzania, East Africa: implications for the stability of cratonic lithosphere. *Journal of Geophysical Research*, **103**, 21201–21213.

ROBERTS, G. G. & WHITE, N. 2010. Estimating uplift rate histories from river profiles using African examples. *Journal of Geophysical Research*, **115**, B02406, doi: 10.1029/2009JB006692.

RYCHERT, C. A., SHEARER, P. M. & FISCHER, K. M. 2010. Scattered wave imaging of the lithosphere–asthenosphere boundary. *Lithos*, **120**, 173–185.

SAVAGE, B. & SILVER, P. G. 2008. Evidence for a compositional boundary within the lithospheric mantle beneath the Kalahari craton from S receiver functions. *Earth and Planetary Science Letters*, **272**, 600–609.

SEBAI, A., STUTZMANN, E., MONTAGNER, J.-P., SICILIA, D. & BEUCLER, E. 2006. Anisotropic structure of the African upper mantle from Rayleigh and Love wave tomography. *Physics of the Earth and Planetary Interiors*, **155**, 48–62.

SEBER, D., SANDVOL, E., SANDVOL, C., BRINDISI, C. & BARAZANGI, M. 2001. Crustal model for the Middle East and North Africa region: implications for the isostatic compensation mechanism. *Geophysical Journal International*, **147**, 630–638.

SHACKLETON, R. 1986. Precambrian collision tectonics in Africa. *In*: COWARD, M. P. & RIES, A. C. (eds) *Collision Tectonics*. Geological Society, London, Special Publications, **19**, 329–349.

SICILIA, D., MONTAGNER, J. P. ET AL. 2008. Upper mantle structure of shear-waves velocities and stratification of anisotropy in the Afar Hotspot region. *Tectonophysics*, **462**, 164–177.

SILVER, P. & CHAN, G. 1991. Shear wave splitting and subcontinental mantle deformation. *Journal of Geophysical Research*, **96**, 16429–16454.

SILVER, P. G., GAO, S. S. & LIU, K. H. (THE KAAPVAAL SEISMIC GROUP). 2001. Mantle deformation beneath Southern Africa. *Geophysics Research Letters*, **28**, 2493–2496.

SIMMONS, N. A., FORTE, A. M. & GRAND, S. P. 2007. Thermochemical structure and dynamics of the African superplume. *Geophysics Research Letters*, **34**, L02301, doi: 10.1029/2006GL028009.

SIMMONS, N. A., FORTE, A. M. & GRAND, S. P. 2009. Joint seismic, geodynamic and mineral physical constraints on three-dimensional mantle heterogeneity: implications for the relative importance of thermal v. compositional heterogeneity. *Geophysical Journal International*, **177**, 1284–1304.

SIMMONS, N. A., FORTE, A. M., BOSCHI, L. & GRAND, S. P. 2010. GyPSuM: A joint tomographic model of mantle density and seismic wave speeds. *Journal of Geophysical Research*, **115**, B12310, doi: 10.1029/2010JB007631.

SPIEGEL, C., KOHN, B. P., BELTON, D. X. & GLEADOW, A. J. W. 2007. Morphotectonic evolution of the central Kenya rift flanks: implications for late Cenozoic environmental change in East Africa. *Geology*, **35**, 427–430.

STANKIEWICZ, J., CHEVROT, S., VAN DER HILST, R. D. & DE WIT, M. J. 2002. Crustal thickness, discontinuity depth, and upper mantle structure beneath southern Africa: constraints from body wave conversions. *Physics of the Earth and Planetary Interiors*, **130**, 235–251.

STUART, G. W., FAIRHEAD, J. D., DORBATH, L. & DORBATH, C. 1985. A seismic refraction study of the crustal structure associated with the Adamawa Plateau and Garoua Rift, Cameroon, West Africa. *Geophysical Journal of the Royal Astronomical Society*, **81**, 1–12.

STUART, G. W., BASTOW, I. D. & EBINGER, C. J. 2006. Crustal structure of the northern Main Ethiopian rift from receiver function studies. *In*: YIRGU, G., EBINGER, C. J. & MAGUIRE, P. K. H. (eds) *The Afar Volcanic Province within the East African Rift System*. Geological Society, London, Special Publications, **253**, 271–293.

TAPLEY, B., RIES, J. ET AL. 2005. GGM02 – an improved Earth gravity field model. *Journal of Geodynamics*, **79**, 467–478.

TEIXELL, A., ARBOLEYA, M.-L., JULIVERT, M. & CHARROUD, M. 2003. Tectonic shortening and topography in the central High Atlas (Morocco). *Tectonics*, **22**, 1051, doi: 10.1029/2002TC001460.

TEIXELL, A., AZARZA, P., ZEYEN, H., FERNÀNDEZ, M. & ARBOLEYA, M.-L. 2005. Effects of mantle upwelling in a compressional setting: the Atlas Mountains of Morocco. *Terra Nova*, **17**, 456–461.

TIBI, R., LARSON, A. M. ET AL. 2005. A broadband seismological investigation of the Cameroon Volcanic Line. *Eos, Transactions, American Geophysical Union*, **86** (Abstract S11B-0170).

TINKER, J., DE WIT, M. & BROWN, R. 2008. Linking source and sink: evaluating the balance between onshore erosion and offshore sediment accumulation since Gondwana break-up, South Africa. *Tectonophysics*, **455**, 94–103.

TOKAM, A.-P. K., TABOD, C. T., NYBLADE, A. A., JULIÀ, J., WIENS, D. A. & PASYANOS, M. E. 2010. Structure of the crust beneath Cameroon, West Africa, from the joint inversion of Rayleigh wave group velocities and receiver functions. *Geophysical Journal International*, **183**, 1061–1076.

VANDECAR, J. C., JAMES, D. E. & ASSUMPÇÃO, M. 1995. Seismic evidence for a fossil mantle plume beneath

South America and implications for plate driving forces. *Nature*, **378**, 25–31.

VINNIK, L., ORESHIN, S., KOSAREV, G., KISELEV, S. & MAKEYEVA, L. 2009. Mantle anomalies beneath southern Africa: evidence from seismic S and P receiver functions. *Geophysical Journal International*, **179**, 279–298.

WALKER, K., NYBLADE, A., KLEMPERER, S., BOKELMANN, G. & OWENS, T. 2004. On the relationship between extension and anisotropy: constraints from shear wave splitting across the East African Plateau. *Journal of Geophysical Research*, **109**, B083202, doi: 10.1029/2003JB002866.

WANG, Y., WEN, L. & WEIDNER, D. 2008. Upper mantle SH- and P- velocity structures and compositional models beneath southern Africa. *Earth and Planetary Science Letters*, **267**, 596–608.

WEBB, S. J., CAWTHORN, R. G., NGUURI, T. & JAMES, D. 2004. Gravity modeling of Bushveld Complex connectivity supported by Southern African Seismic Experiment results. *South African Journal of Geology*, **107**, 207–218.

WEERARATNE, D. S., FORSYTH, D. W., FISCHER, K. M. & NYBLADE, A. A. 2003. Evidence for an upper mantle plume beneath the Tanzanian craton from Rayleigh wave tomography. *Journal of Geophysical Research*, **108**, 2427, doi: 10.1029/2001JB001225.

WHALER, K. A. & HAUTOT, S. 2006. The electrical resistivity structure of the crust beneath the northern Ethiopian rift. *In*: YIRGU, G., EBINGER, C. J. & MAGUIRE, P. K. H. (eds) *The Afar Volcanic Province within the East African Rift System*. Geological Society, London, Special Publications, **256**, 293–305.

WILSON, M. & GUIRAUD, R. 1992. Magmatism and rifting in Western and Central Africa, from Late Jurassic to Recent times. *Tectonophysics*, **213**, 203–225.

WITTLINGER, G. & FARRA, V. 2007. Converted waves reveal a thick and layered tectosphere beneath the Kalahari super-craton. *Earth and Planetary Science Letters*, **254**, 404–415.

WÖLBERN, I., RÜMPKER, G., SCHUMANN, A. & MUWANGA, A. 2010. Crustal thinning beneath the Rwenzori region, Albertine rift, Uganda, from receiver-function analysis. *International Journal of Earth Sciences*, **99**, 1545–1557.

YANG, Y., LI, A. & RITZWOLLER, M. H. 2008. Crustal and uppermost mantle structure in southern Africa revealed from ambient noise and teleseismic tomography. *Geophysical Journal International*, **174**, 235–248.

ZEYEN, H., AYARZA, P., FERNÀNDEZ, M. & RIMI, A. 2005. Lithospheric structure under the western African–European plate boundary: a transect across the Atlas Mountains and the Gulf of Cadiz. *Tectonics*, **24**, doi: 10.1029/2004TC001639.

ZHU & KANAMORI 2000. Moho depth variation in southern California from teleseismic receiver functions. *Journal of Geophysical Research*, **105**, 2969–2980.